Progress on the spectroscopy study of the composite Higgs model with Sp(4) gauge theory and multiple fermion representations

02.08.2024 @ University of Liverpool

LATTICE 2024 LIVERPOOL

Ho Hsiao, C.-J. David Lin

Jong-Wan Lee

부산대학교 PUSAN NATIONAL UNIVERSITY Deog Ki Hong

UNIVERSITY OF PLYMOUTH Davide Vadacchino

Swansea University Prifysgol Abertawe

Ed Bennett, Niccolò Forzano, Biagio Lucini, Maurizio Piai, Fabian Zierler

Outline

- Introduction:
  - Sp(4) gauge theory: A Composite Higgs model
  - Top partner
- Techniques
  - Smearing, GEVP, Scale setting: gradient-flow
- Results
- Summary and Outlook

Composite Higgs Model

Scales:

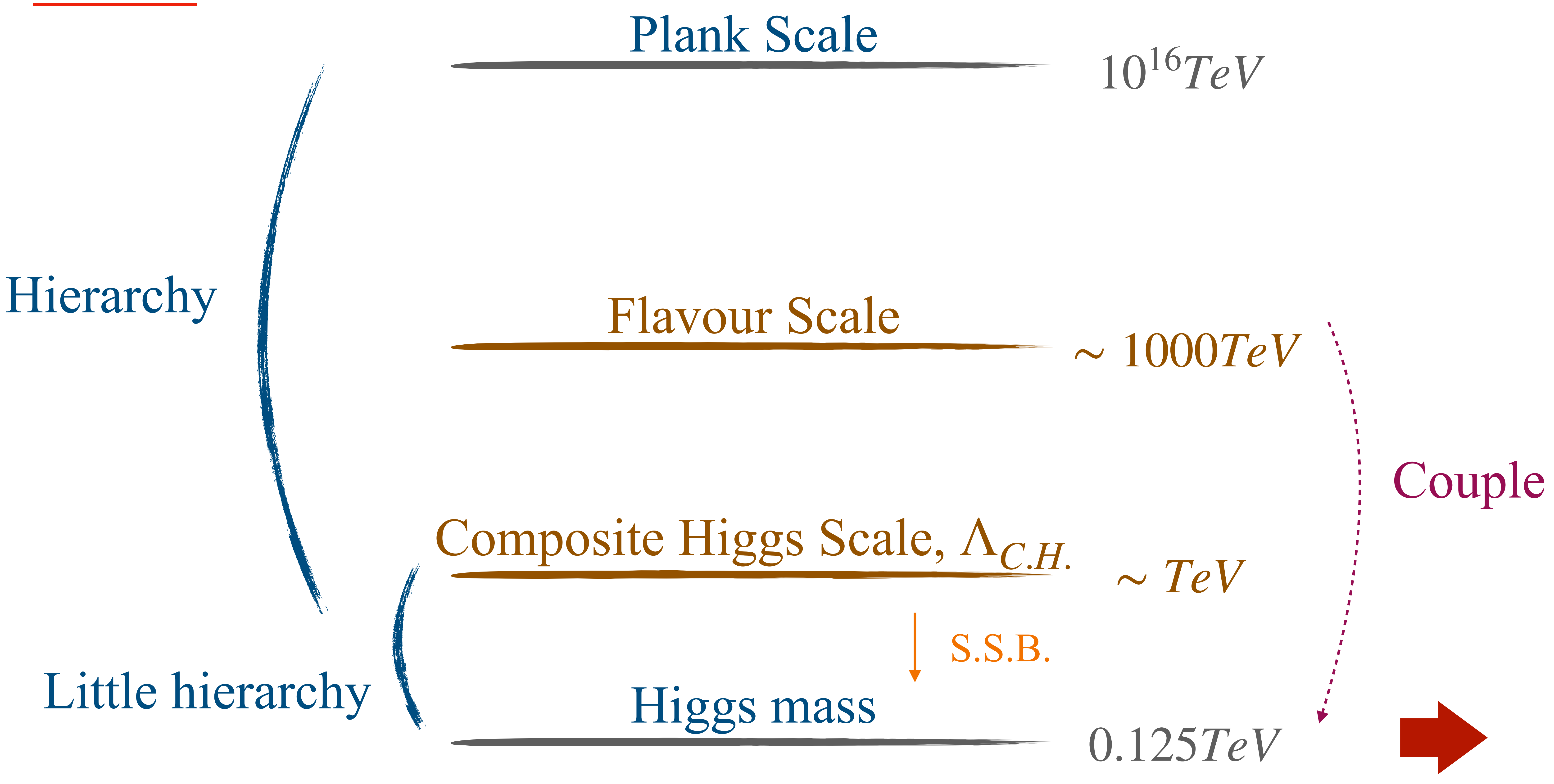

Higgs boson as a bound state of new strong dynamics, which is lighter because of being a pseudo Nambu-Goldstone Boson.

Composite Higgs Model

Composite Higgs Model

Symmetries

Composite Higgs Model

Symmetries

- Global symmetry: $\mathcal{G}$

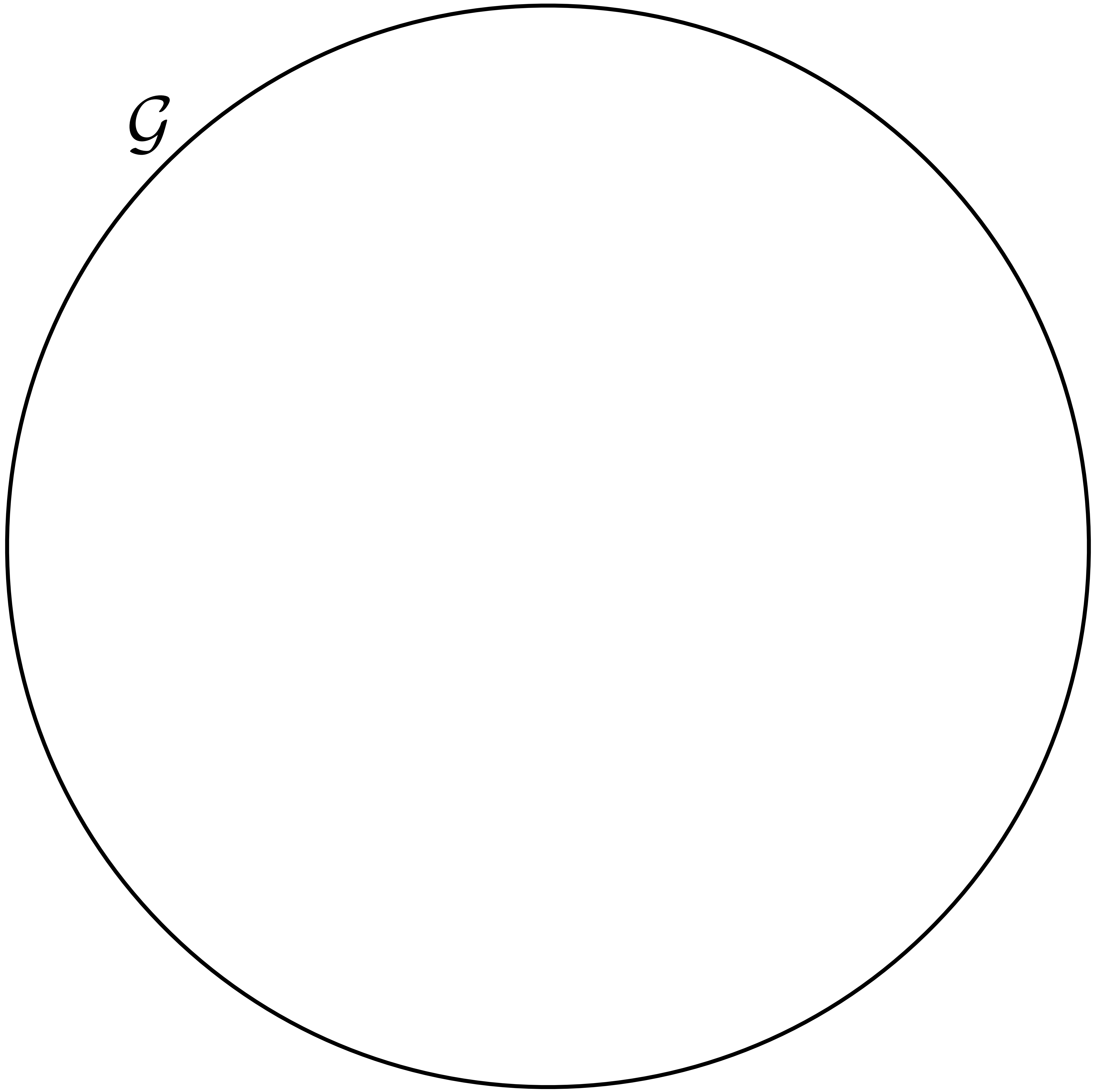

Composite Higgs Model

Symmetries

- Global symmetry: $\mathcal{G}$
- Subgroup: $\mathcal{H}$ with $G_{\mathrm{EW}} \subset \mathcal{H}$

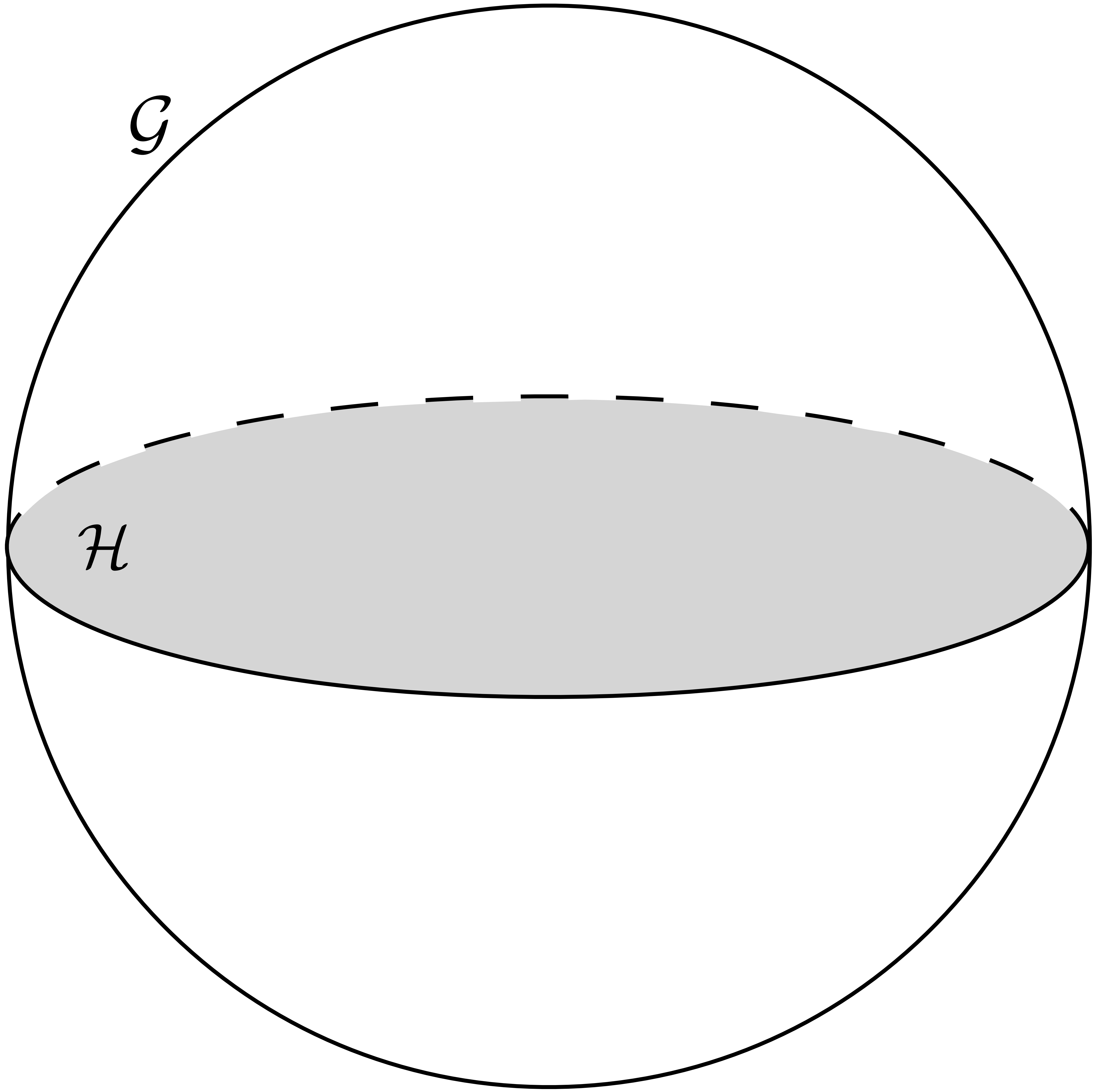

Composite Higgs Model

Symmetries

- Global symmetry: $\mathcal{G}$
- Subgroup: $\mathcal{H}$ with $G_{\mathrm{EW}} \subset \mathcal{H}$

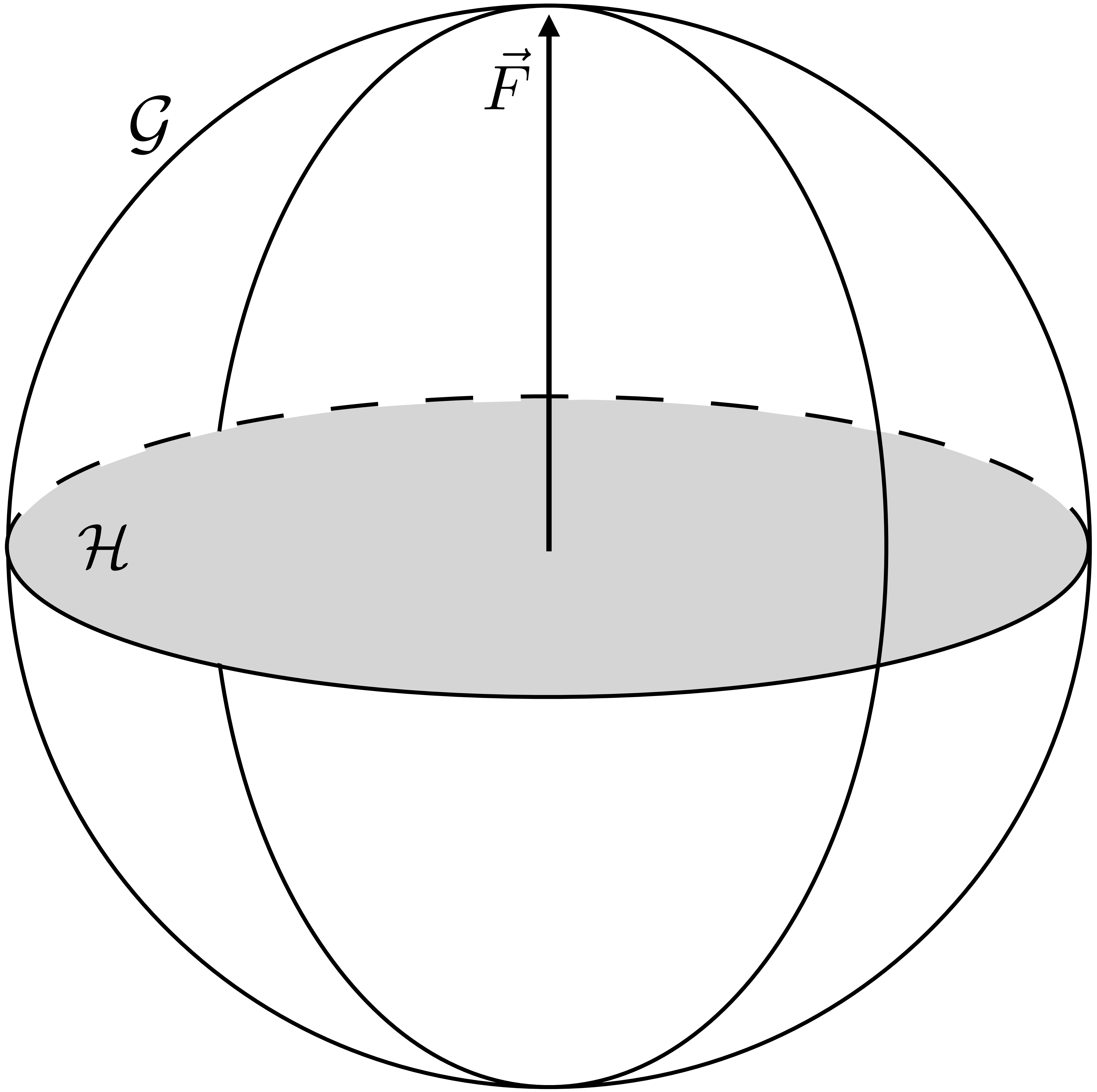

Composite Higgs Model

Symmetries

- Global symmetry: $\mathcal{G}$
- Subgroup: $\mathcal{H}$ with $G_{\mathrm{EW}} \subset \mathcal{H}$
- Vacuum misalignment angle: θ_B

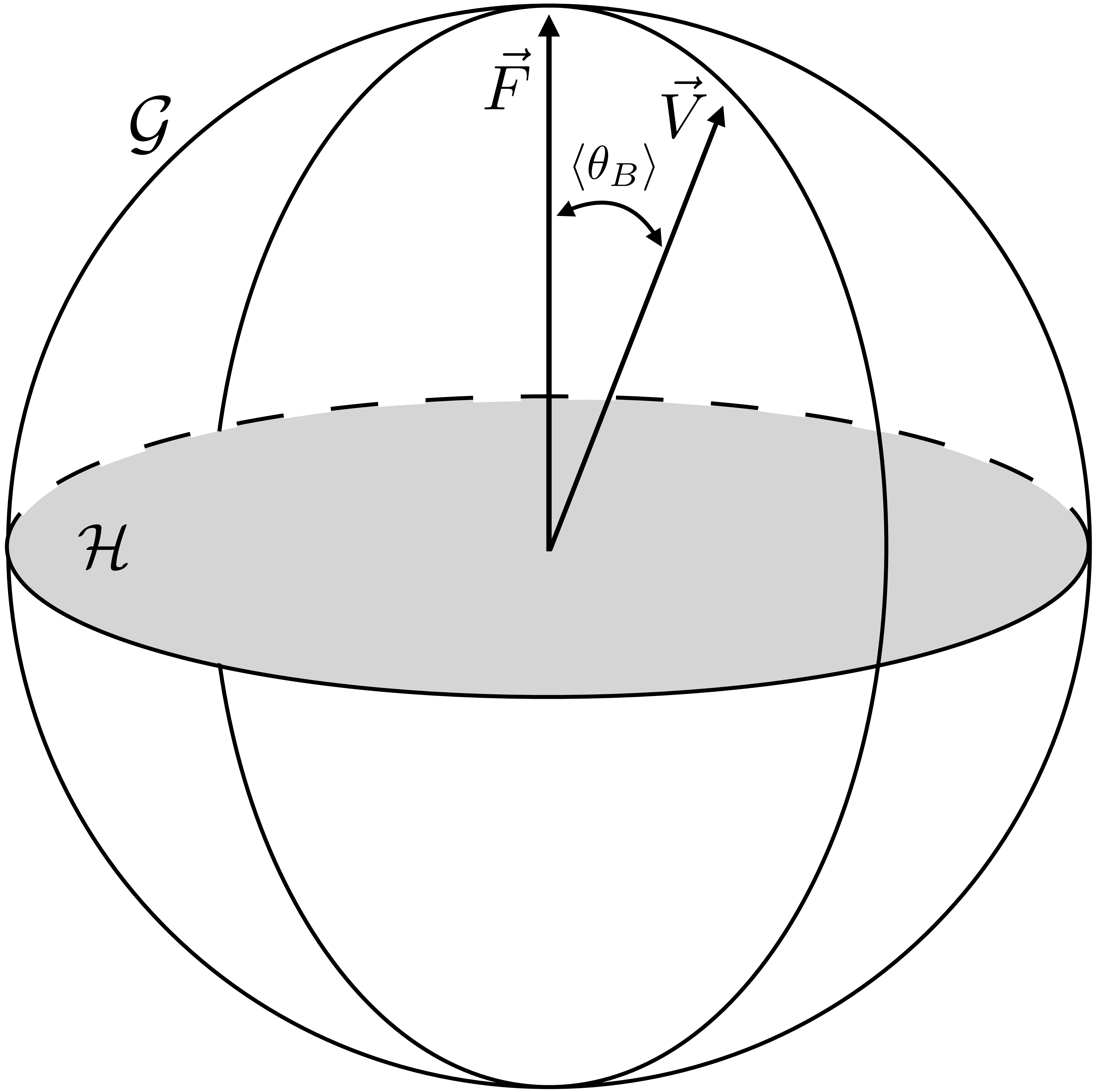

Composite Higgs Model

Symmetries

- Global symmetry: $\mathcal{G}$
- Subgroup: $\mathcal{H}$ with $G_{\mathrm{EW}} \subset \mathcal{H}$
- Vacuum misalignment angle: θ_B
- Coset $\mathcal{G}/\mathcal{H} \to$ pNGBs

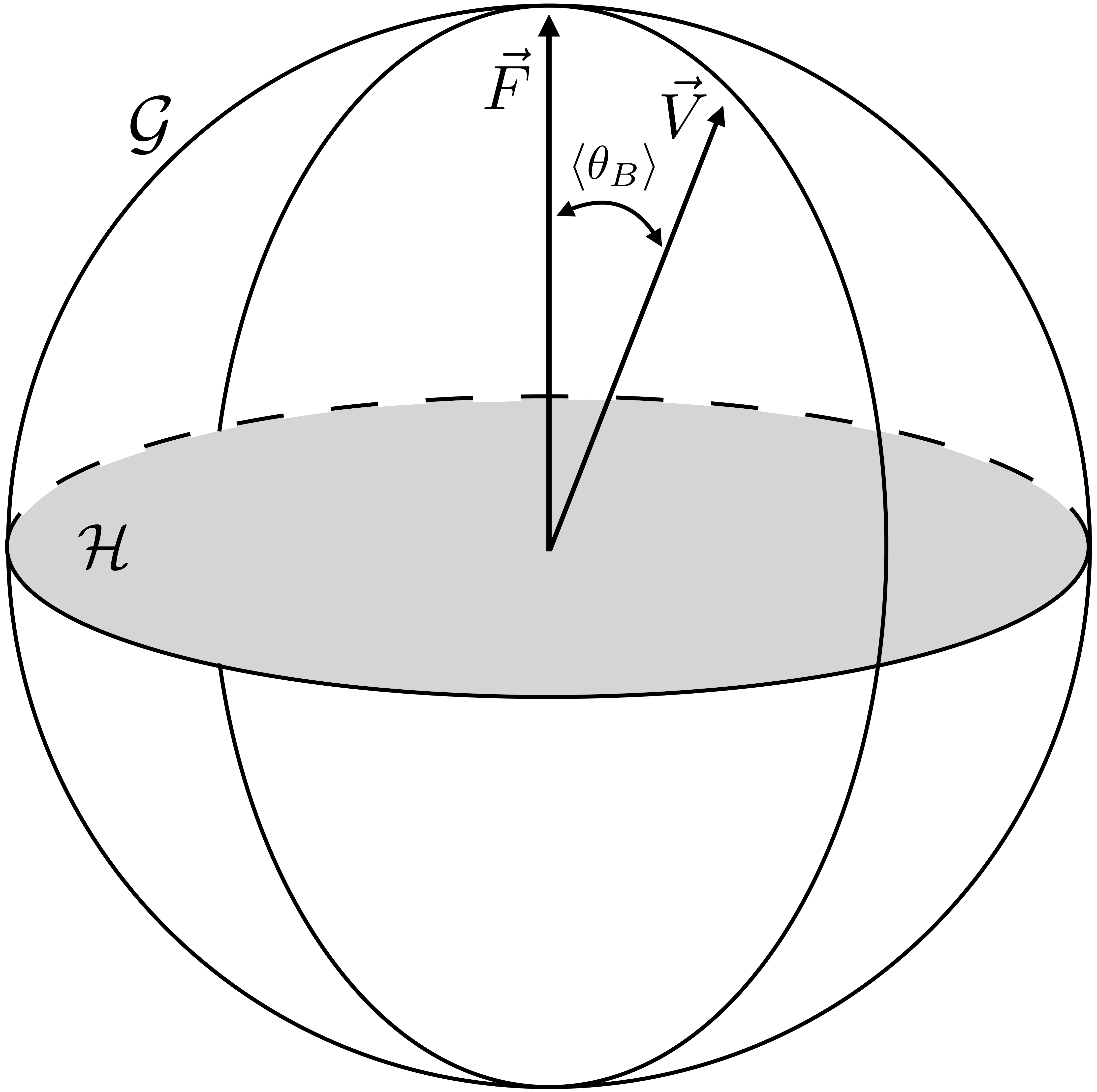

Composite Higgs Model

<u>Symmetries</u>

- Global symmetry: $\mathcal{G}$
- Subgroup: $\mathcal{H}$ with $G_{\mathrm{EW}} \subset \mathcal{H}$
- Vacuum misalignment angle: θ_B
- Coset $\mathcal{G}/\mathcal{H} \to$ pNGBs
- The scale of the EWSB: $v = f \sin\theta_B \;\; (f = |\vec{F}|)$

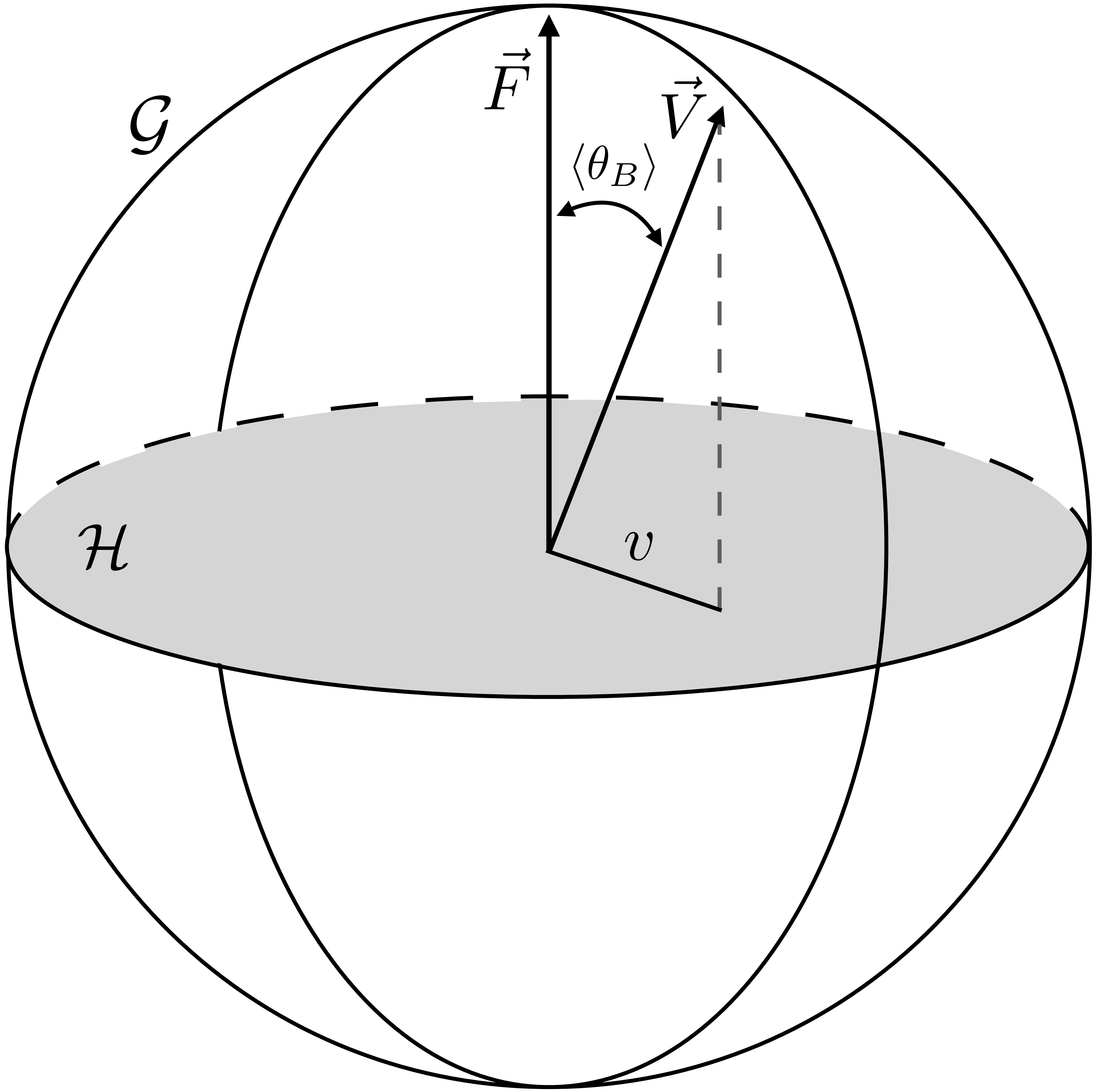

Composite Higgs Model

Symmetries

- Global symmetry: $\mathcal{G}$
- Subgroup: $\mathcal{H}$ with $G_{\mathrm{EW}} \subset \mathcal{H}$
- Vacuum misalignment angle: θ_B
- Coset $\mathcal{G}/\mathcal{H} \to$ pNGBs
- The scale of the EWSB: $v = f \sin\theta_B \; (f = |\vec{F}|)$

❖ Technicolor model: Higgs $\in \mathcal{H}$

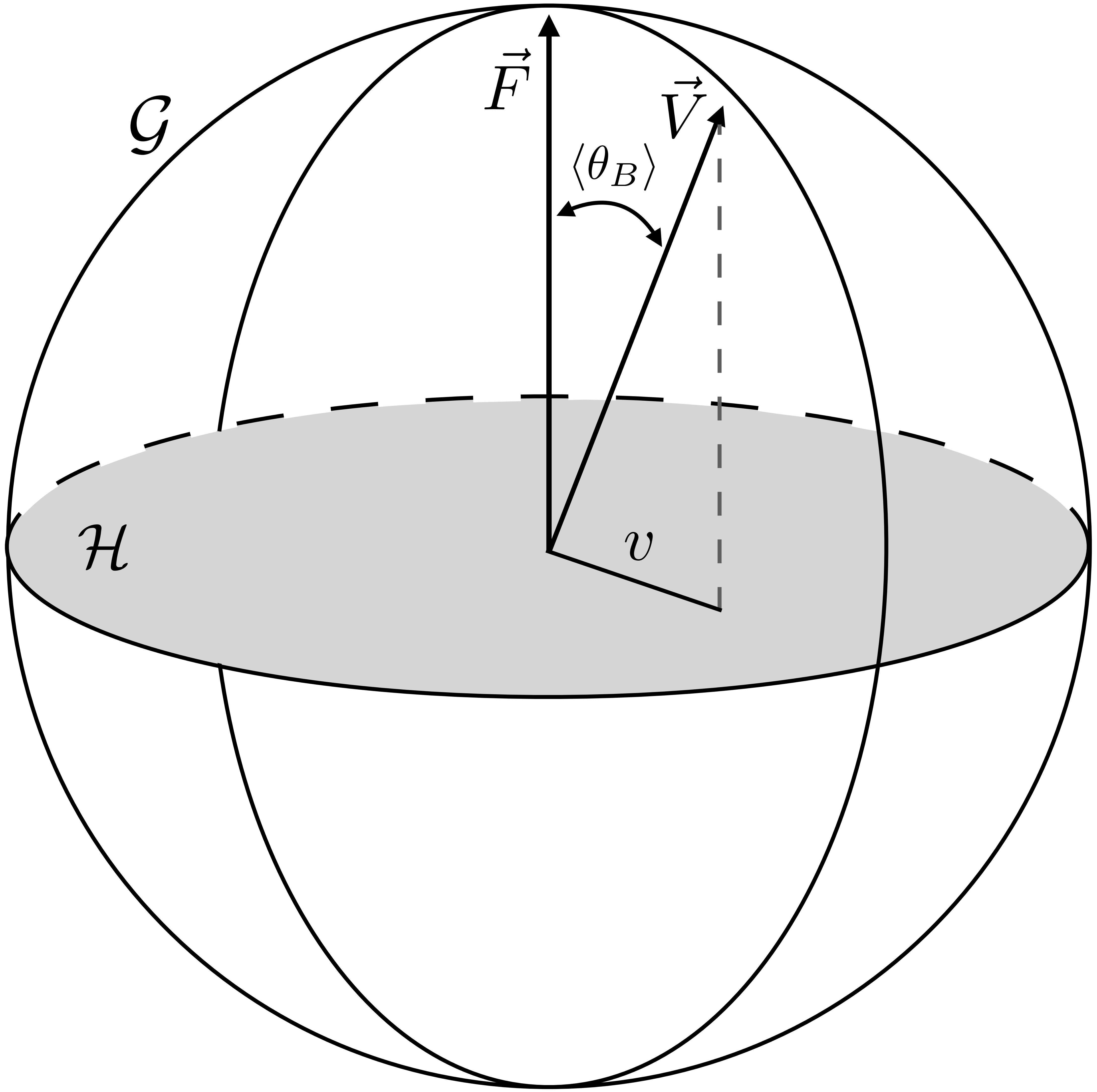

Composite Higgs Model

Top partial compositeness

Composite Higgs Model

Top partial compositeness

Top partners:

Composite Higgs Model

Top partial compositeness

Top partners:

- Share the same quantum number as the top

Composite Higgs Model

Top partial compositeness

Top partners:

- Share the same quantum number as the top
  - Spin-1/2 bound states emerging from the novel strong-interaction sector

Composite Higgs Model

Top partial compositeness

Top partners:

- Share the same quantum number as the top
  - Spin-1/2 bound states emerging from the novel strong-interaction sector
  - Carry QCD colour charge

Composite Higgs Model

Top partial compositeness

Top partners:

- Share the same quantum number as the top
  - Spin-1/2 bound states emerging from the novel strong-interaction sector
  - Carry QCD colour charge
- Hypercolour-neutral

Composite Higgs Model

Top partial compositeness

Top partners:

- Share the same quantum number as the top
  - Spin-1/2 bound states emerging from the novel strong-interaction sector
  - Carry QCD colour charge

➡ Introducing higher representation

- Hypercolour-neutral

Composite Higgs Model

Top partial compositeness

Top partners:

- Share the same quantum number as the top
  - Spin-1/2 bound states emerging from the novel strong-interaction sector
  - Carry QCD colour charge

➡ Introducing higher representation

- Hypercolour-neutral
- Give the mass to the top by mixing with it

$$\mathcal{L}_{\text{mass}} = -M\bar{T}_L T_R - y\frac{v}{\sqrt{2}}\bar{t}_L T_R - \lambda f \bar{T}_L t_R + \text{h.c.}\,, \qquad \Rightarrow m_t \simeq \frac{yv}{\sqrt{2}}\frac{\lambda f}{\sqrt{\lambda^2 f^2 + M^2}}\,.$$

$$= (\bar{t}_L \quad \bar{T}_L)\begin{pmatrix} 0 & \frac{yv}{\sqrt{2}} \\ \lambda f & M \end{pmatrix}\begin{pmatrix} t_R \\ T_R \end{pmatrix} + \text{h.c.}\,.$$

Composite Higgs Models

*Weyl fermions

Name	Gauge group	ψ	χ	Baryon type
M1	$SO(7)$	$5\times\mathbf{F}$	$6\times\mathbf{Spin}$	$\psi\chi\chi$
M2	$SO(9)$	$5\times\mathbf{F}$	$6\times\mathbf{Spin}$	$\psi\chi\chi$
M3	$SO(7)$	$5\times\mathbf{Spin}$	$6\times\mathbf{F}$	$\psi\psi\chi$
M4	$SO(9)$	$5\times\mathbf{Spin}$	$6\times\mathbf{F}$	$\psi\psi\chi$
M5	$Sp(4)$	$5\times\mathbf{A}_2$	$6\times\mathbf{F}$	$\psi\chi\chi$
M6	$SU(4)$	$5\times\mathbf{A}_2$	$3\times(\mathbf{F},\overline{\mathbf{F}})$	$\psi\chi\chi$
M7	$SO(10)$	$5\times\mathbf{F}$	$3\times(\mathbf{Spin},\overline{\mathbf{Spin}})$	$\psi\chi\chi$
M8	$Sp(4)$	$4\times\mathbf{F}$	$6\times\mathbf{A}_2$	$\psi\psi\chi$
M9	$SO(11)$	$4\times\mathbf{Spin}$	$6\times\mathbf{F}$	$\psi\psi\chi$
M10	$SO(10)$	$4\times(\mathbf{Spin},\overline{\mathbf{Spin}})$	$6\times\mathbf{F}$	$\psi\psi\chi$
M11	$SU(4)$	$4\times(\mathbf{F},\overline{\mathbf{F}})$	$6\times\mathbf{A}_2$	$\psi\psi\chi$
M12	$SU(5)$	$4\times(\mathbf{F},\overline{\mathbf{F}})$	$3\times(\mathbf{A}_2,\overline{\mathbf{A}_2})$	$\psi\psi\chi,\ \psi\chi\chi$

[D. Franzosi and G. Ferretti, arXiv:1905.08273]

Composite Higgs Models

*Weyl fermions

Name	Gauge group	ψ	χ	Baryon type
M1	$SO(7)$	$5 \times \mathbf{F}$	$6 \times \mathbf{Spin}$	$\psi\chi\chi$
M2	$SO(9)$	$5 \times \mathbf{F}$	$6 \times \mathbf{Spin}$	$\psi\chi\chi$
M3	$SO(7)$	$5 \times \mathbf{Spin}$	$6 \times \mathbf{F}$	$\psi\psi\chi$
M4	$SO(9)$	$5 \times \mathbf{Spin}$	$6 \times \mathbf{F}$	$\psi\psi\chi$
M5	$Sp(4)$	$5 \times \mathbf{A}_2$	$6 \times \mathbf{F}$	$\psi\chi\chi$
M6	$SU(4)$	$5 \times \mathbf{A}_2$	$3 \times (\mathbf{F}, \overline{\mathbf{F}})$	$\psi\chi\chi$
M7	$SO(10)$	$5 \times \mathbf{F}$	$3 \times (\mathbf{Spin}, \overline{\mathbf{Spin}})$	$\psi\chi\chi$
M8	$Sp(4)$	$4 \times \mathbf{F}$	$6 \times \mathbf{A}_2$	$\psi\psi\chi$
M9	$SO(11)$	$4 \times \mathbf{Spin}$	$6 \times \mathbf{F}$	$\psi\psi\chi$
M10	$SO(10)$	$4 \times (\mathbf{Spin}, \overline{\mathbf{Spin}})$	$6 \times \mathbf{F}$	$\psi\psi\chi$
M11	$SU(4)$	$4 \times (\mathbf{F}, \overline{\mathbf{F}})$	$6 \times \mathbf{A}_2$	$\psi\psi\chi$
M12	$SU(5)$	$4 \times (\mathbf{F}, \overline{\mathbf{F}})$	$3 \times (\mathbf{A}_2, \overline{\mathbf{A}_2})$	$\psi\psi\chi$, $\psi\chi\chi$

[D. Franzosi and G. Ferretti, arXiv:1905.08273]

Composite Higgs Models

*Weyl fermions

Name	Gauge group	ψ	χ	Baryon type
M1	$SO(7)$	$5 \times \mathbf{F}$	$6 \times \mathbf{Spin}$	$\psi\chi\chi$
M2	$SO(9)$	$5 \times \mathbf{F}$	$6 \times \mathbf{Spin}$	$\psi\chi\chi$
M3	$SO(7)$	$5 \times \mathbf{Spin}$	$6 \times \mathbf{F}$	$\psi\psi\chi$
M4	$SO(9)$	$5 \times \mathbf{Spin}$	$6 \times \mathbf{F}$	$\psi\psi\chi$
M5	$Sp(4)$	$5 \times \mathbf{A}_2$	$6 \times \mathbf{F}$	$\psi\chi\chi$
M6	$SU(4)$	$5 \times \mathbf{A}_2$	$3 \times (\mathbf{F}, \overline{\mathbf{F}})$	$\psi\chi\chi$
M7	$SO(10)$	$5 \times \mathbf{F}$	$3 \times (\mathbf{Spin}, \overline{\mathbf{Spin}})$	$\psi\chi\chi$
M8	$Sp(4)$	$4 \times \mathbf{F}$	$6 \times \mathbf{A}_2$	$\psi\psi\chi$
M9	$SO(11)$	[redacted]	[redacted]	$\psi\psi\chi$
M10	$SO(10)$	[redacted]	[redacted]	$\psi\psi\chi$
M11	$SU(4)$	[redacted]	[redacted]	$\psi\psi\chi$
M12	$SU(5)$	$4 \times (\mathbf{F}, \overline{\mathbf{F}})$	$3 \times (\mathbf{A}_2, \overline{\mathbf{A}_2})$	$\psi\psi\chi$, $\psi\chi\chi$

The minimal model

[Barnard et al, arXiv:1311.6562]

[D. Franzosi and G. Ferretti, arXiv:1905.08273]

Our choice of model

- Sp(4) gauge theory with 2F+3AS Dirac fermions

(4F+6AS 2-component Weyl fermions)

- Breaking pattern:

$$G/H = SU(4)\times SU(6)\ /\ Sp(4)\times SO(6)$$

Enhanced global symmetry due to the (pseudo-) reality

Our choice of model

- Sp(4) gauge theory with 2F+3AS Dirac fermions

  (4F+6AS 2-component Weyl fermions)

- Breaking pattern:

$$G/H = SU(4)\times SU(6)\ /\ Sp(4)\times SO(6)$$

Enhanced global symmetry due to the (pseudo-) reality

- $SU(4)/Sp(4)$ gives 5 goldstone bosons.
  - 4: SM Higgs doublet
  - 1: made heavy in model building

Our choice of model

- Sp(4) gauge theory with 2F+3AS Dirac fermions

  (4F+6AS 2-component Weyl fermions)

- Breaking pattern:

$$G/H = SU(4)\times SU(6) \,/\, Sp(4)\times SO(6)$$

Enhanced global symmetry due to the (pseudo-) reality

$SU(4)/Sp(4)$ gives 5 goldstone bosons.

- 4: SM Higgs doublet
- 1: made heavy in model building

SU(3) embedded in antisymmetric representation:

$$SU(6) \rightarrow SO(6) \supset SU(3)$$

→ QCD colour SU(3)

Chimera Baryon

a, b, c: hypercolour, Ω: 4×4 symplectic matrix
J: spin, R: irreducible rep. of the fundamental sector

- Interpolating operators

  - Λ type: $\mathcal{O}^{5}_{\mathrm{CB}} = \left(\bar{\psi}^{1\,a} C \gamma^{5} \psi^{2\,b}\right) \Omega_{ad} \Omega_{bc} \chi^{k\,cd}$

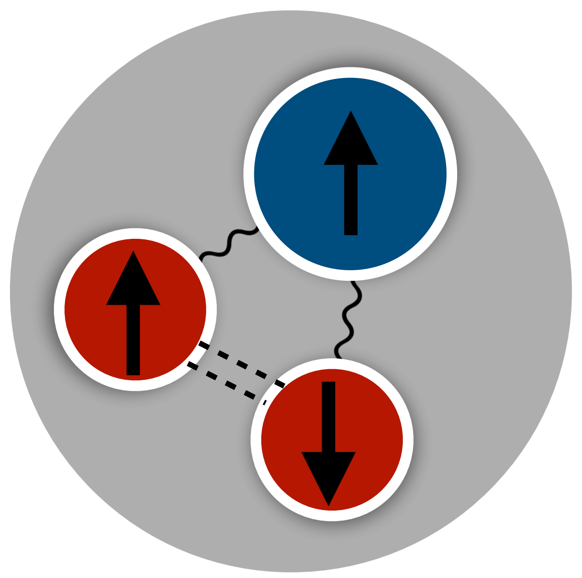

$(J, R) = (1/2, 5)$
*top partner

  - Σ type: $\mathcal{O}^{i}_{\mathrm{CB}} = \left(\bar{\psi}^{1\,a} C \gamma^{i} \psi^{2\,b}\right) \Omega_{ad} \Omega_{bc} \chi^{k\,cd}$

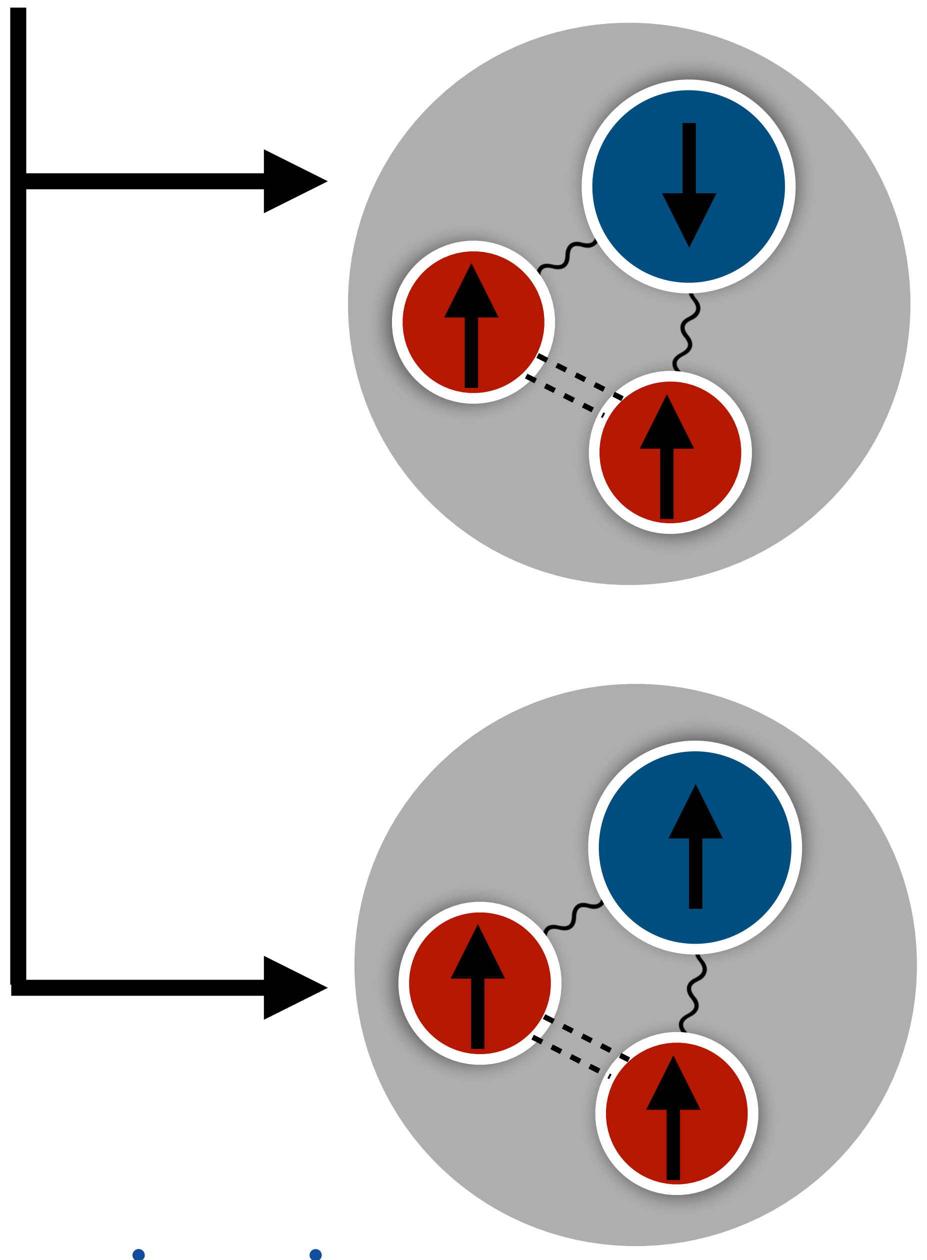

Σ: $(J, R) = (1/2, 10)$
*top partner

Σ^*: $(J, R) = (3/2, 10)$

Parity projection

$$P_e \equiv \frac{1}{2}(1 + \gamma^0) \text{ and } P_o \equiv \frac{1}{2}(1 - \gamma^0)$$

Spin projection

$$\left(P^{1/2}\right)^{ij} = \frac{1}{3}\gamma^i \gamma^j \text{ and } \left(P^{3/2}\right)^{ij} = \delta^{ij} - \frac{1}{3}\gamma^i \gamma^j$$

Mesons

Label M	Interpolating operator $\mathcal{O}_{\mathrm{M}}$	Mesons in $N_f = 2$ QCD	J^P	$Sp(4)$	$SO(6)$
PS	$\overline{Q^i}\gamma_5 Q^j$	π	0^-	5	1
S	$\overline{Q^i} Q^J$	a_0	0^+	5	1
V	$\overline{Q^i}\gamma_\mu Q^j$	ρ	1^-	10	1
T	$\overline{Q^i}\gamma_0\gamma_\mu Q^j$	ρ	1^-	10	1
AV	$\overline{Q^i}\gamma_5\gamma_\mu Q^j$	a_1	1^+	5	1
AT	$\overline{Q^i}\gamma_5\gamma_0\gamma_\mu Q^j$	b_1	1^+	10	1
ps	$\overline{\Psi^k}\gamma_5 \Psi^l$	π	0^-	1	$20'$
s	$\overline{\Psi^k} \Psi^l$	a_0	0^+	1	$20'$
v	$\overline{\Psi^k}\gamma_\mu \Psi^l$	ρ	1^-	1	15
t	$\overline{\Psi^k}\gamma_0\gamma_\mu \Psi^l$	ρ	1^-	1	15
av	$\overline{\Psi^k}\gamma_5\gamma_\mu \Psi^l$	a_1	1^+	1	$20'$
at	$\overline{\Psi^k}\gamma_5\gamma_0\gamma_\mu \Psi^l$	b_1	1^+	1	15

Lattice Method

- The action: $S = S_g + S_f$

$$S_g \equiv \beta \sum_x \sum_{\mu<\nu} \left(1 - \frac{1}{2N} \mathrm{Re}\,\mathrm{Tr}\, U_\mu(x) U_\nu(x+\hat{\mu}) U_\mu^\dagger(x+\hat{\nu}) U_\nu^\dagger(x) \right),$$

$$S_f \equiv a^4 \sum_{j=1}^{N_f} \sum_x \overline{Q}^j(x) D_m^{(\mathrm{f})} Q^j(x) + a^4 \sum_{j=1}^{n_f} \sum_x \overline{\Psi}^j(x) D_m^{(as)} \Psi^j(x)$$

- Software
  - HiRep [L. D. Debbio et al.]
  - GRID [P. Boyle et al.]
- Wilson fermion

Lattice Method

Smearing techniques

Lattice Method

Smearing techniques

- Wuppertal smearing (Gaussian smearing) acts on fermion field increasing the overlap of ground state.

$$q^{(n+1)}(x) = \frac{1}{1+2d\varepsilon}\left[q^{(n)}(x) + \varepsilon \sum_{\mu=\pm 1}^{\pm d} U_\mu(x) q^{(n)}(x+\hat{\mu})\right]$$

Lattice Method

Smearing techniques

- Wuppertal smearing (Gaussian smearing) acts on fermion field increasing the overlap of ground state.

$$q^{(n+1)}(x) = \frac{1}{1+2d\varepsilon}\left[q^{(n)}(x) + \varepsilon \sum_{\mu=\pm 1}^{\pm d} U_\mu(x) q^{(n)}(x+\hat{\mu})\right]$$

- APE smearing averages out UV fluctuations of the gauge fields.

$$U_\mu^{(n+1)}(x) = P\left\{(1-\alpha)U_\mu^{(n)}(x) + \frac{\alpha}{6} S_\mu^{(n)}(x)\right\}, \quad S_\mu(x) = \sum_{\pm\nu\neq\mu} U_\nu(x) U_\mu(x+\hat{\nu}) U_\nu^\dagger(x+\hat{\mu})$$

Lattice Method

GEVP

- Generalised Eigenvalue problem

$$C(t_2)v_n(t_2, t_1) = \lambda_n(t_2, t_1)C(t_1)v_n(t_2, t_1) \to \lambda_n(t_2, t_1)$$

The matrix $C(t)$ is constructed by different interpolating operators.

Lattice Method

GEVP

- Generalised Eigenvalue problem

$$C(t_2)v_n(t_2, t_1) = \lambda_n(t_2, t_1)C(t_1)v_n(t_2, t_1) \to \lambda_n(t_2, t_1)$$

The matrix $C(t)$ is constructed by different interpolating operators.

- Type I: vary the operators by V, T, and their cross-channels

$$C(t) = \begin{pmatrix} c_{VV}(t) & c_{VT}(t) \\ c_{TV}(t) & c_{TT}(t) \end{pmatrix}$$

$$\Rightarrow E_n(t) = \ln\left[\frac{\lambda_n(t+a, t_0)}{\lambda_n(t, t_0)}\right]$$

Lattice Method

GEVP

- Generalised Eigenvalue problem

$$C(t_2)v_n(t_2,t_1) = \lambda_n(t_2,t_1)C(t_1)v_n(t_2,t_1) \to \lambda_n(t_2,t_1)$$

The matrix $C(t)$ is constructed by different interpolating operators.

- Type I: vary the operators by V, T, and their cross-channels

$$C(t) = \begin{pmatrix} c_{VV}(t) & c_{VT}(t) \\ c_{TV}(t) & c_{TT}(t) \end{pmatrix}$$

$$\Rightarrow E_n(t) = \ln\left[\frac{\lambda_n(t+a,t_0)}{\lambda_n(t,t_0)}\right]$$

- Type II: vary smearing levels with a single channel

$$\mathcal{C}_{\mathcal{O}}(t) = \begin{pmatrix} C_{\mathcal{O}}^{0,\,0}(t) & C_{\mathcal{O}}^{0,\,40}(t) & C_{\mathcal{O}}^{0,\,80}(t) \\ C_{\mathcal{O}}^{40,\,0}(t) & C_{\mathcal{O}}^{40,\,40}(t) & C_{\mathcal{O}}^{40,\,80}(t) \\ C_{\mathcal{O}}^{80,\,0}(t) & C_{\mathcal{O}}^{80,\,40}(t) & C_{\mathcal{O}}^{80,\,80}(t) \end{pmatrix}$$

$$\Rightarrow E_n(t,t_0) = \cosh^{-1}\left[\frac{\lambda_n(t+a,t_0)+\lambda_n(t-a,t_0)}{2\lambda_n(t,t_0)}\right].$$

Lattice Method

Scale setting: gradient-flow

- Lüscher demonstrated that the action density can be related to the renormalised coupling with an extra dimension, *flow time t*:

[Martin Lüscher. 2009]

$$\underbrace{\alpha(\mu)}_{\text{renormalised coupling}} = k_\alpha t^2 \langle E(t) \rangle \equiv \underbrace{k_\alpha}_{\text{analytically computable}} \varepsilon(t) \longrightarrow \varepsilon(t)\,|_{t=t_0} = \varepsilon_0$$

renormalised coupling

analytically computable

$$\Rightarrow W(t) = t\frac{\mathrm{d}\varepsilon(t)}{\mathrm{d}t}$$

with $\mu = 1/\sqrt{8t}$ and $E(t) = -\frac{1}{2}\mathrm{Tr}(G_{\mu\nu}G_{\mu\nu})$.

$$\Rightarrow W(t)\,|_{t=\omega_0^2} = W_0 = 0.28125$$

The gradient flow of the gauge field:

$$\frac{\mathrm{d}B_\mu(t,x)}{\mathrm{d}t} = D_\nu G_{\nu\mu}(t,x), \quad B_\mu(t,x)\,|_{t=0} = A_\mu(t,x)$$

Results: before fully dynamical

Sp(4) gauge [1712.04220]

Review:
Sp(2N) [2304.01070]

- Meson [1911.00437]
- Singlet [2304.07191]

Fund. $N_f = 2$

- Meson [2210.08154]

Anti. $n_f = 3$

Quenched

Fully dynamical

- F. and AS. Meson spectra [1912.06505]
- Glueball [2010.15781]
- Topology [2205.09254, 2205.09364]
- Chimera baryon [2311.14663]
- large-N meson [2312.08465]

- Parameter scan[2202.05516]
- GRID with Sp(2N) [2306.11649]
- Singlet meson [2405.05765]
- Spectral densities [2405.01388]

Results: Mesons

Spectrum

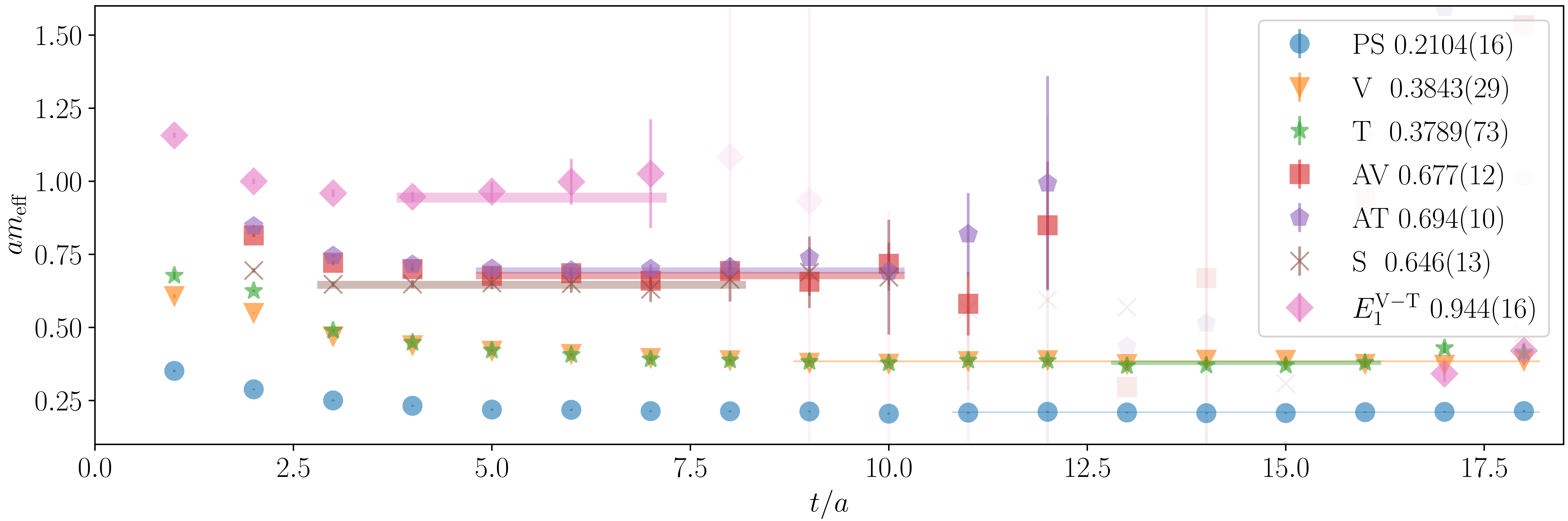

Figure 4.3: The effective mass plot of ensemble DB2M4.

Results: Mesons

Smearing measurements

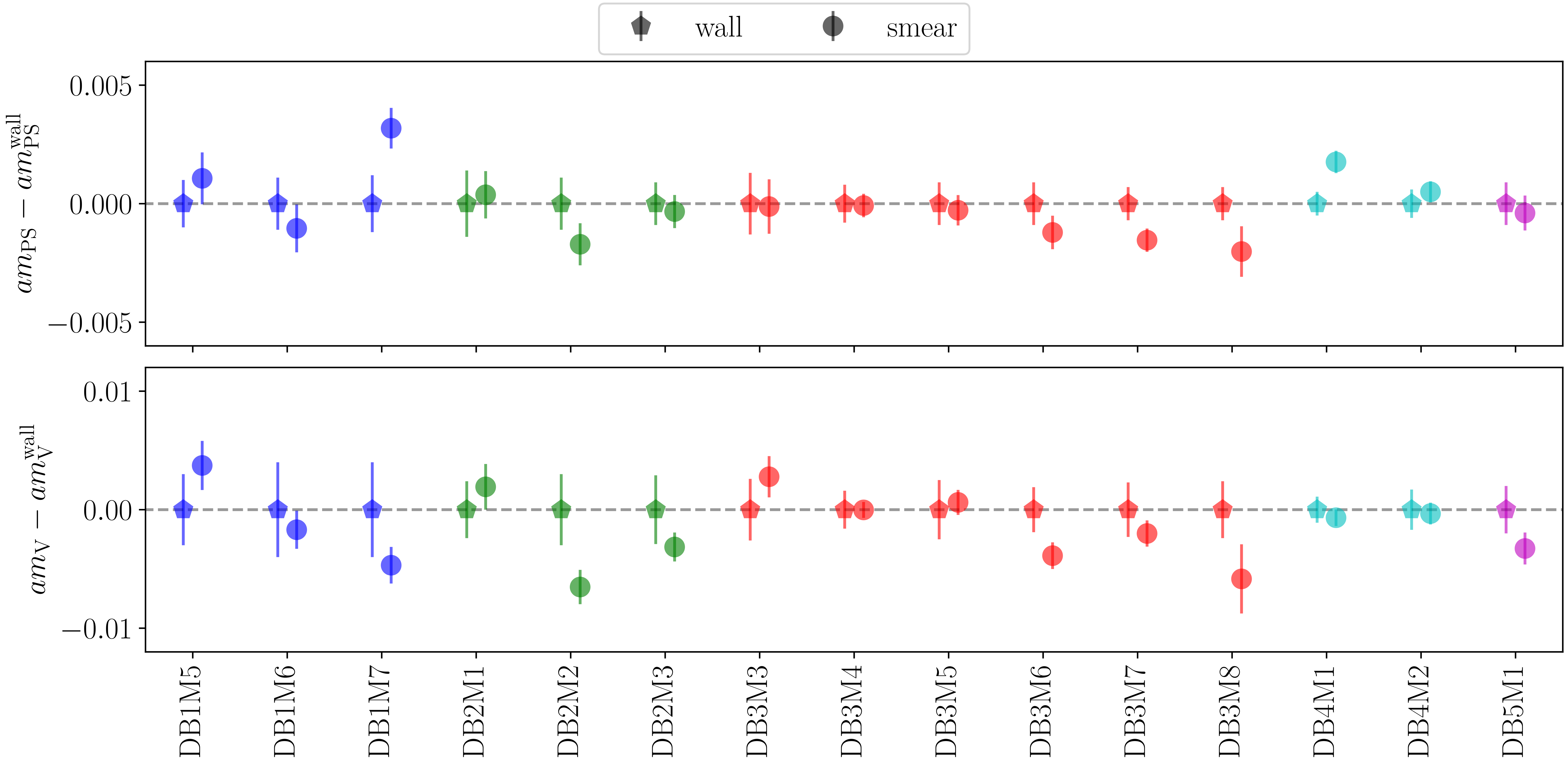

Figure: Comparison of PS (upper panel) and V (lower panel) meson masses with a wall source and a smeared source, measured on (f) dynamical ensembles. The colors indicate the β value: 6.9 (blue), 7.05 (green), 7.2 (red), 7.4 (cyan), and 7.5 (magenta).

Results: Mesons

Chiral EFT and Extrapolations

- Apply tree-level chiral perturbation theory for the continuum and massless extrapolations.

$$\hat{m}_M^{2,\mathrm{NLO}} = \hat{m}_M^{2,\chi}\left(1 + L_M^0 \hat{m}_{\mathrm{PS}}^2\right) + W_M^0 \hat{a}$$

- Quenched results:

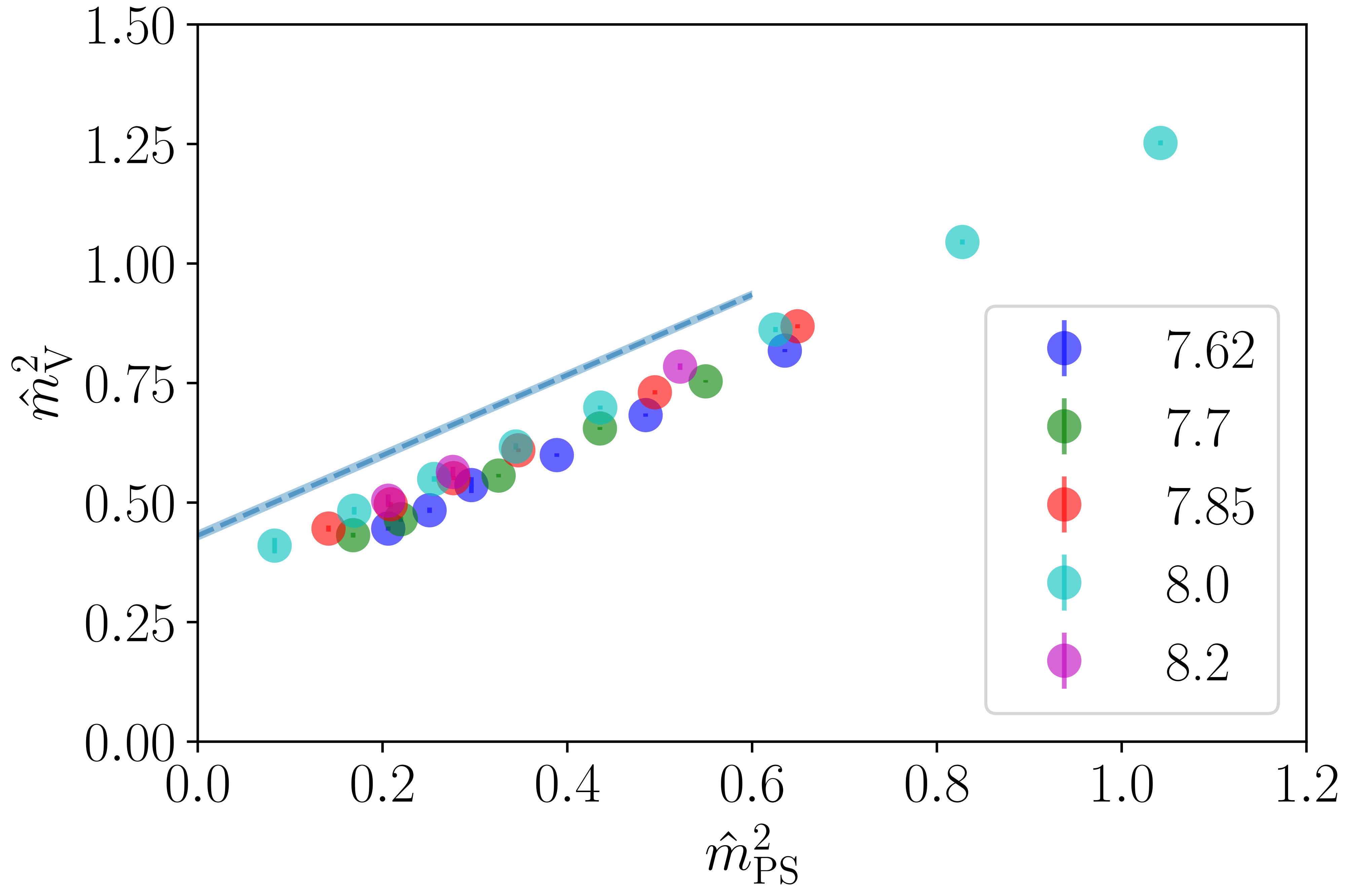

Meson	source	$\hat{m}_M^{2,\chi}$	L_M^0	W_M^0
V	smeared	0.431(11)	1.94(6)	−0.226(16)
	wall	0.451(13)	1.86(7)	−0.257(20)
v	smeared	0.632(18)	1.477(54)	−0.298(29)
	wall	0.657(21)	1.375(56)	−0.336(34)

Results: Mesons

Full Spectrum

- Quenched results:

  - Fundamental (blue)
  - Antisymmetric (red)
  - Glueballs (black)

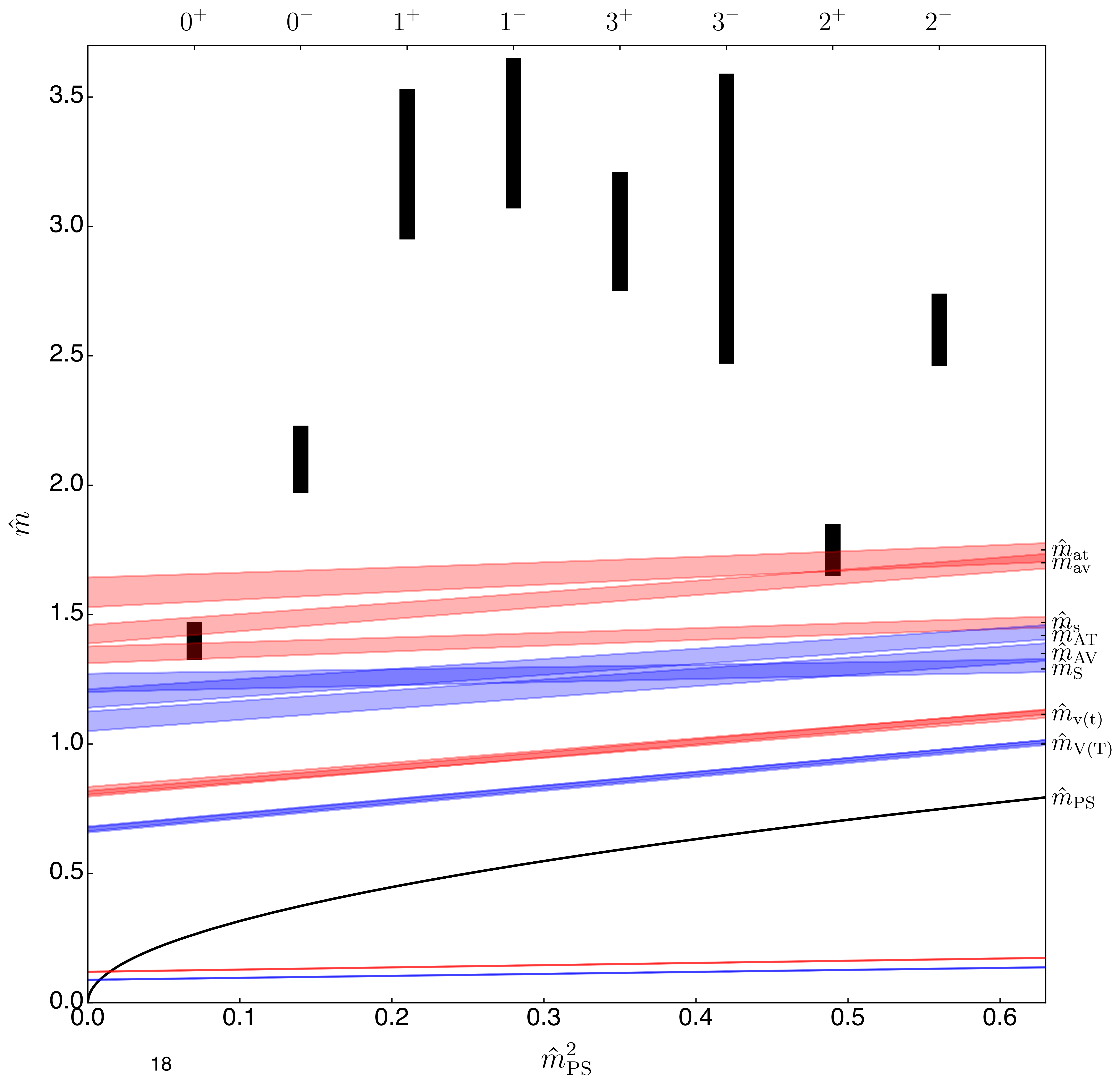

Results: Mesons

Dynamical $N_f = 2$ calculations

- Quenching effects: quenched (blue) vs dynamical (red)

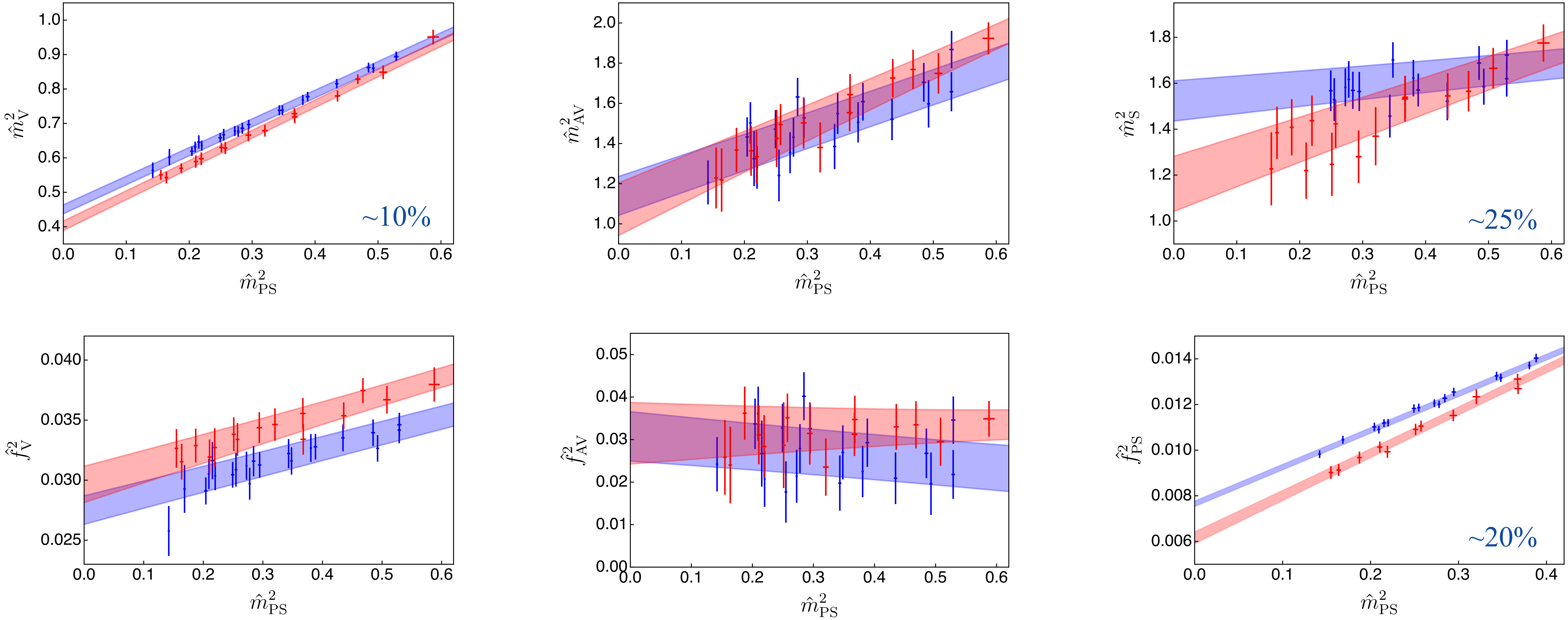

Results: Chimera Baryons

Results: chimera baryons

Fitting

- Quenched results
- Apply tree-level baryon chiral perturbation theory

$$m_{\rm CB} = m^{\chi}_{CB} + F_2\hat{m}^2_{\rm PS} + A_2\hat{m}_{\rm ps}{}^2 + L_1\hat{a} + F_3\hat{m}^3_{\rm PS} + A_3\hat{m}^3_{\rm ps} + L_{2F}\hat{a}\hat{m}^2_{\rm PS} + L_{2A}\hat{a}\hat{m}^2_{\rm ps} + F_4\hat{m}^4_{\rm PS} + A_4\hat{m}^4_{\rm ps} + C_4\hat{m}^2_{\rm PS}\hat{m}^2_{\rm ps}$$

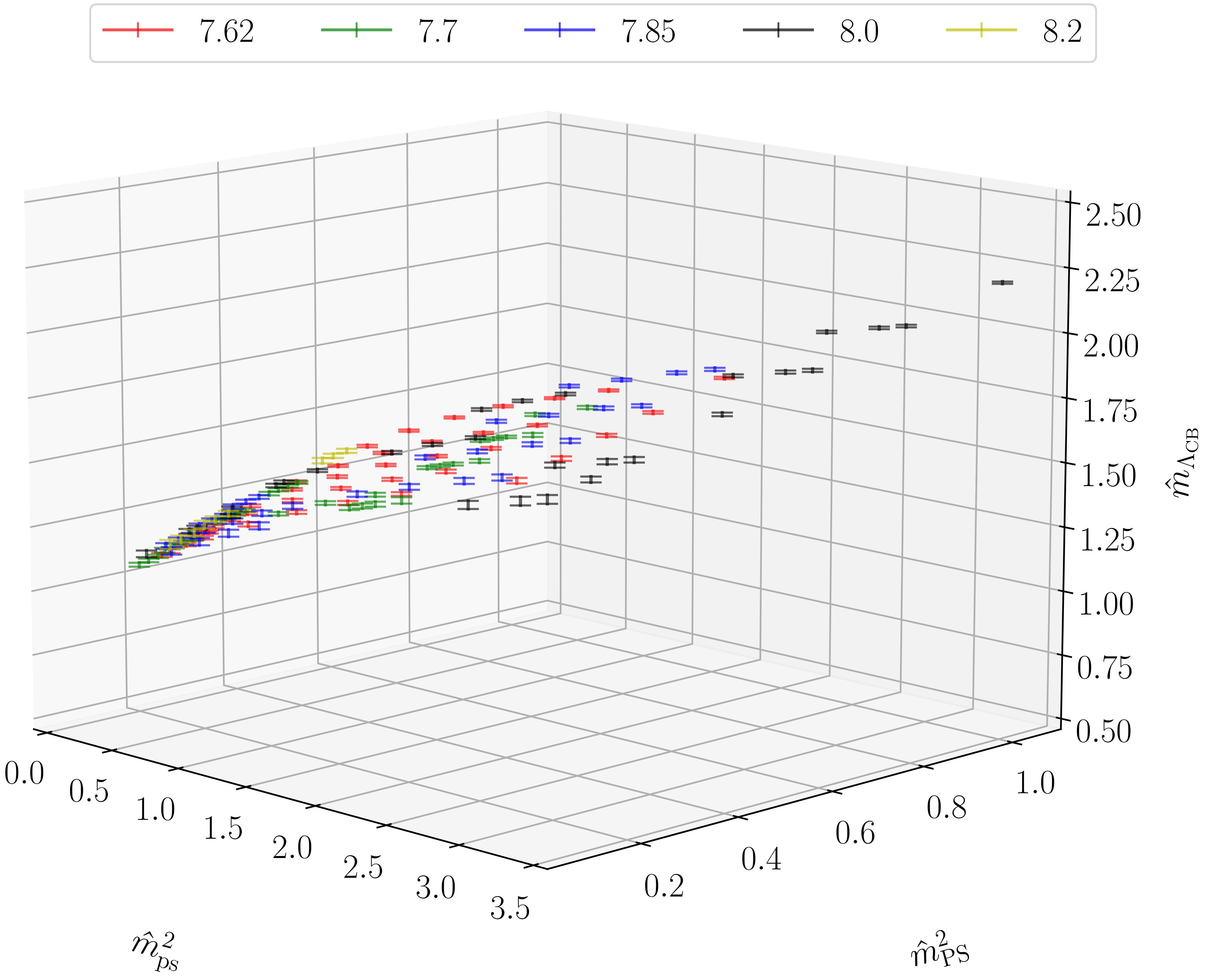

Results: chimera baryons

Massless-continuum limit

Figure: The mass of three chimera baryons, $\Lambda_{\rm CB}$, $\Sigma_{\rm CB}$, and $\Sigma^*_{\rm CB}$, as a function of $\hat{m}^2_{\rm PS}$ (left) and $\hat{m}^2_{\rm ps}$ (right), in the limit where the lattice spacing vanishes, while $\hat{m}^2_{\rm ps}=0$(left) and $\hat{m}^2_{\rm PS}=0$ (right).

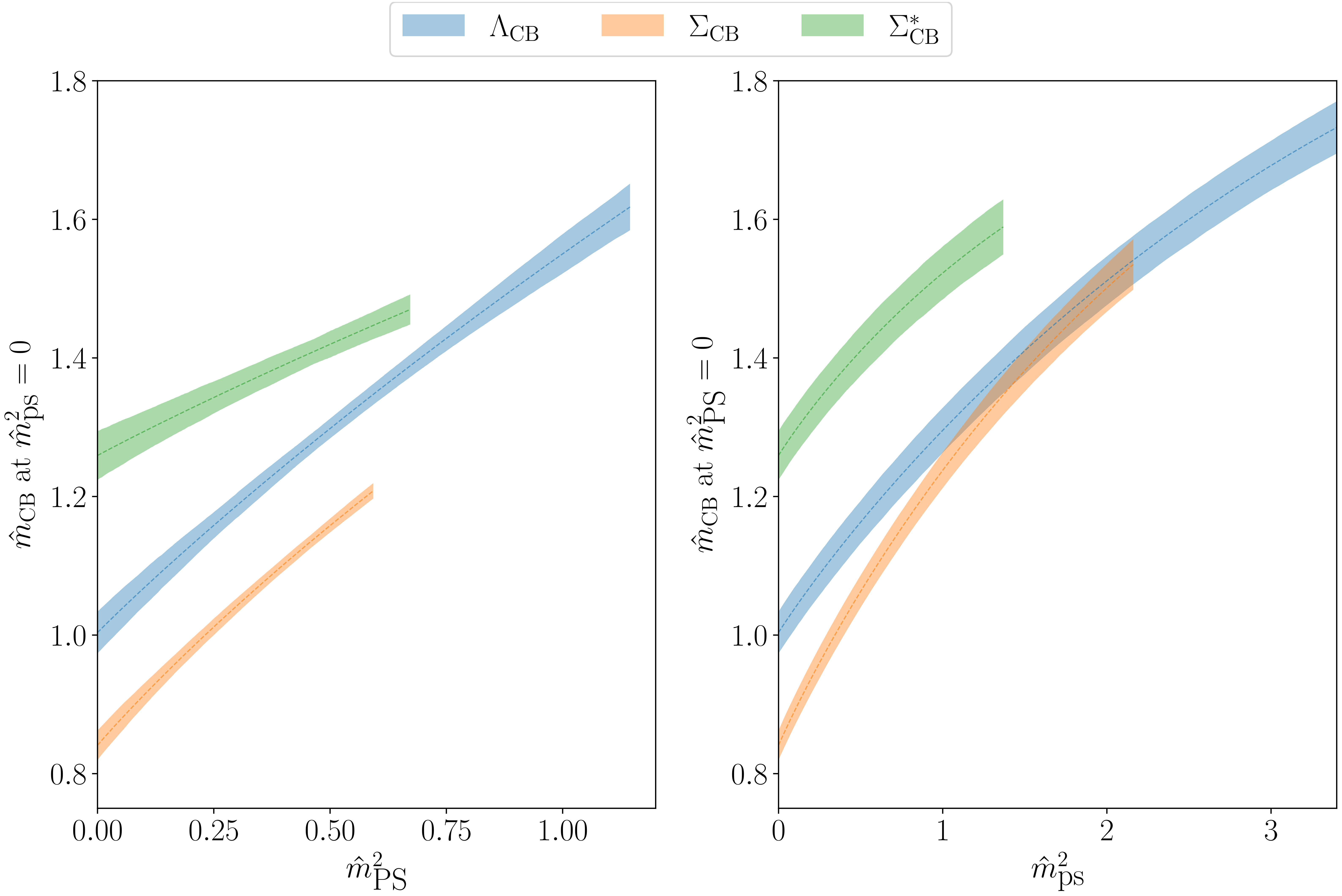

Results: chimera baryons

Massless-continuum limit

Figure: Comparison with masses of mesons in quenched approximation for fermions in the fundamental (blue bands) and antisymmetric (red bands) representation of $Sp(4)$, and glueballs (yellow) at massless-continuum limit.

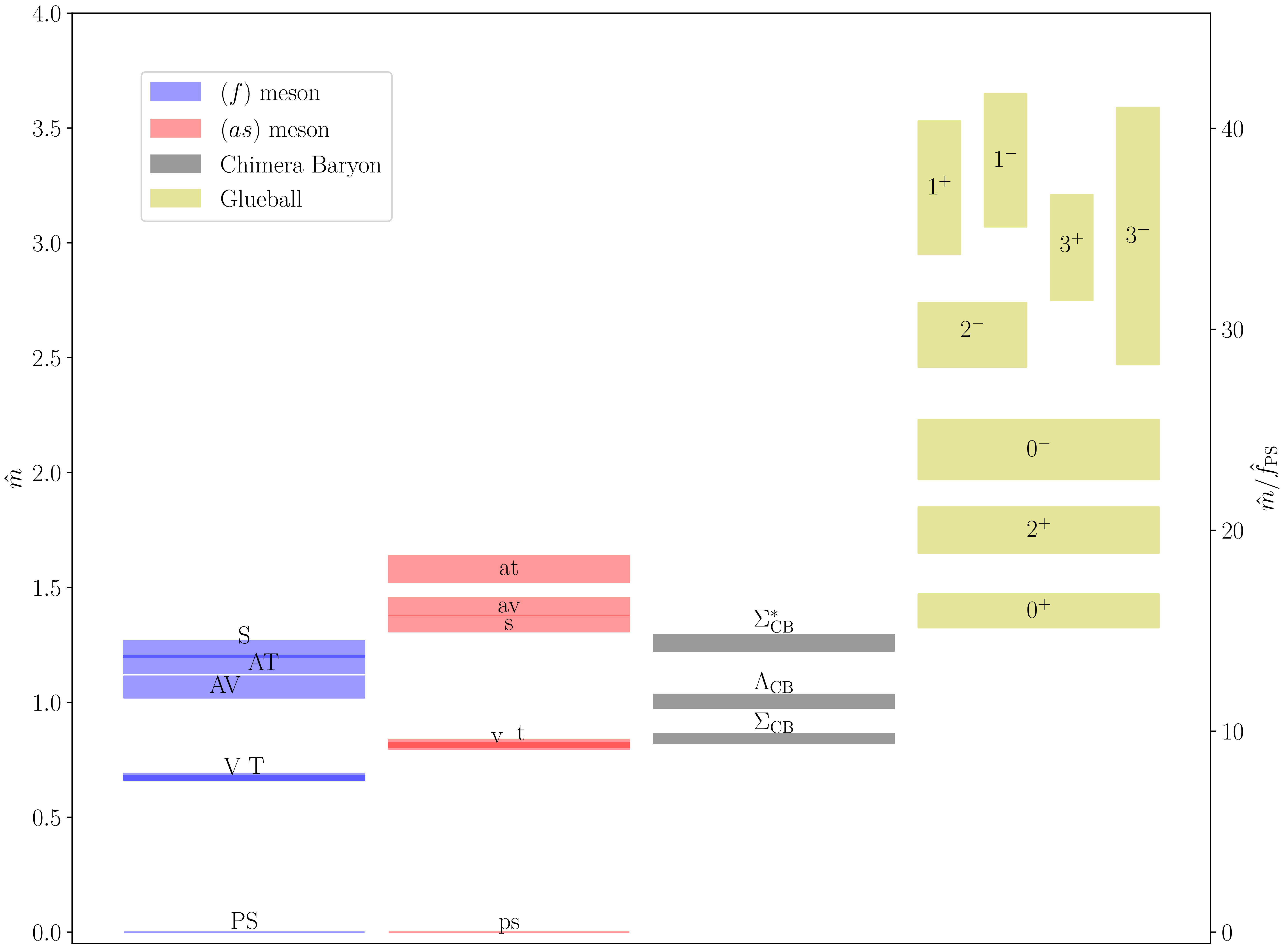

Fully dynamical ensembles

Label	β	$am_0^{(\mathrm{as})}$	$am_0^{(\mathrm{f})}$	$N_t \times N_s$	$\delta_{\mathrm{traj.}}$	$\langle P \rangle$	w_0/a	$m_{\mathrm{PS}}/m_{\mathrm{V}}$	$m_{\mathrm{ps}}/m_{\mathrm{v}}$
M1	6.5	-1.01	-0.71	48 $\times$ 20	14	0.585172(16)	2.5200(50)	0.898(7)	0.925(6)
M2	6.5	-1.01	-0.71	64 $\times$ 20	28	0.585172(12)	2.5300(40)	0.902(5)	0.928(2)
M3	6.5	-1.01	-0.71	96 $\times$ 20	26	0.585156(13)	2.5170(40)	0.898(3)	0.926(2)
M4	6.5	-1.01	-0.70	64 $\times$ 20	20	0.584228(12)	2.3557(31)	0.913(4)	0.935(3)
M5	6.5	-1.01	-0.72	64 $\times$ 32	20	0.5860810(93)	2.6927(31)	0.885(4)	0.931(2)

Results: chimera baryons

Dynamical simulations

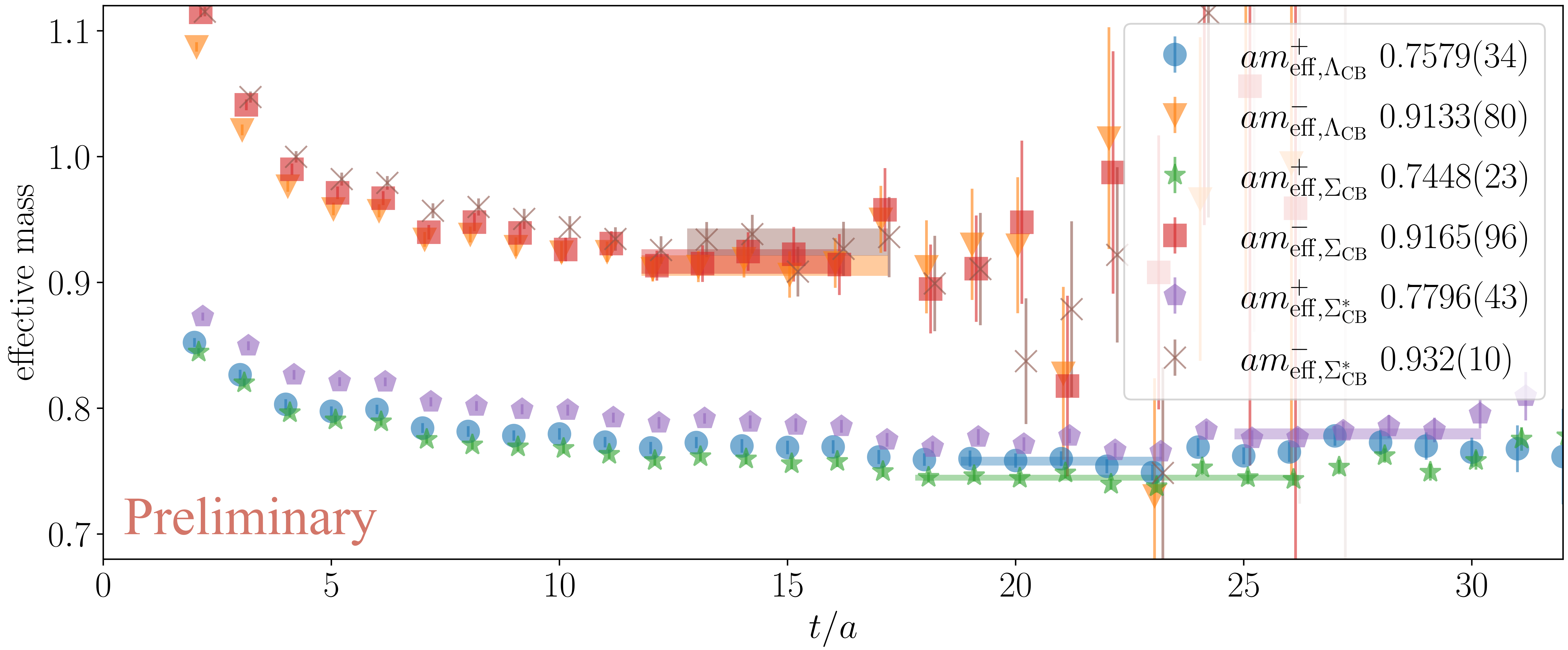

Figure 5.14: Effective mass plots of chimera baryons measured on fully dynamical ensemble M2. The masses displayed in the legend are extracted by solving the GEVP, using various smearing-level operators as the basis.

Results: chimera baryons

Dynamical simulations

Figure: Spectrum of ensemble M4.

$(am_0^{(f)}, am_0^{(as)}) = (-0.70, -1.01)$

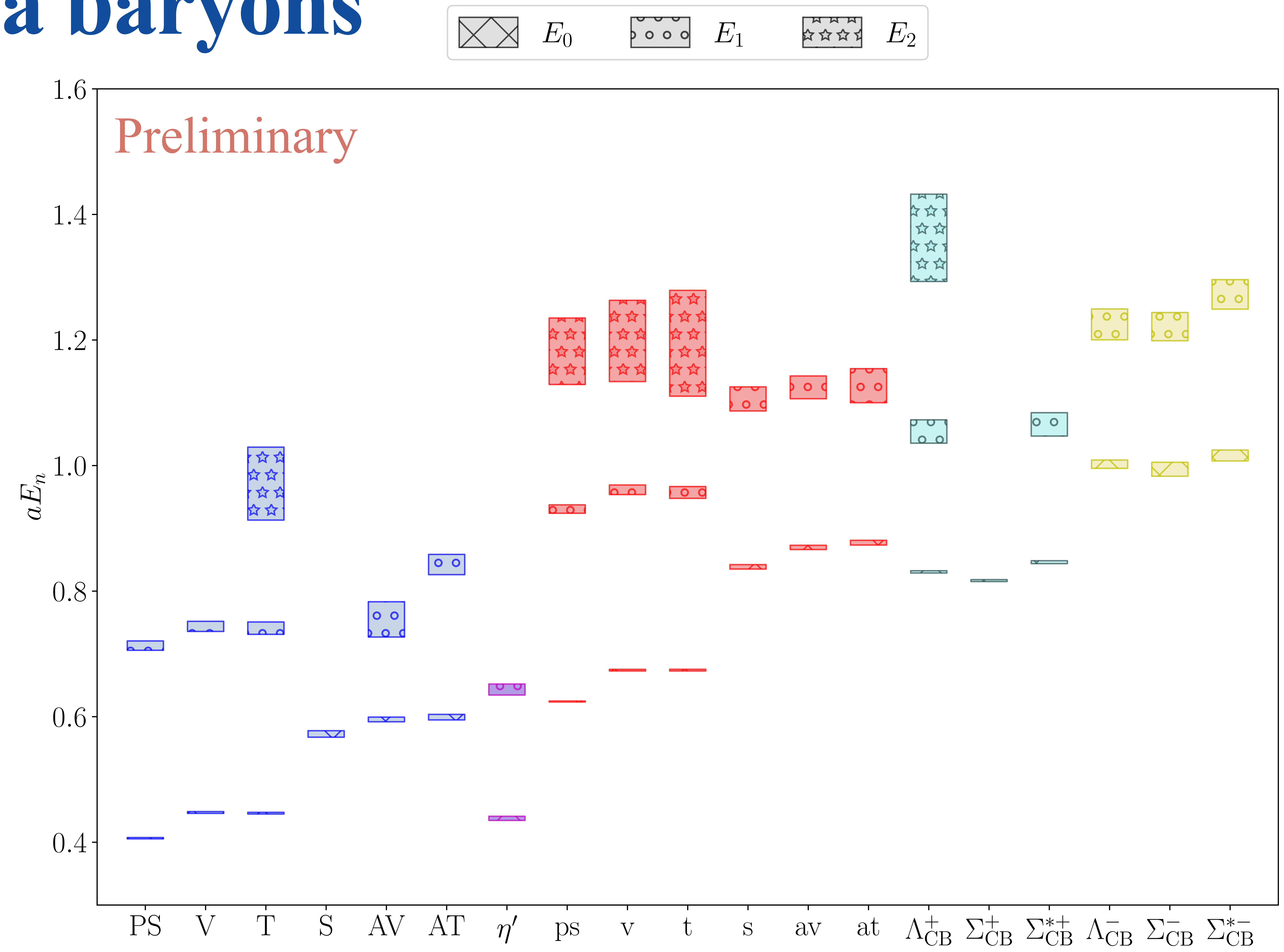

Results: chimera baryons

Dynamical simulations

Figure: spectrum of ensemble M2.

$(am_0^{(f)}, am_0^{(as)}) = (-0.71, -1.01)$

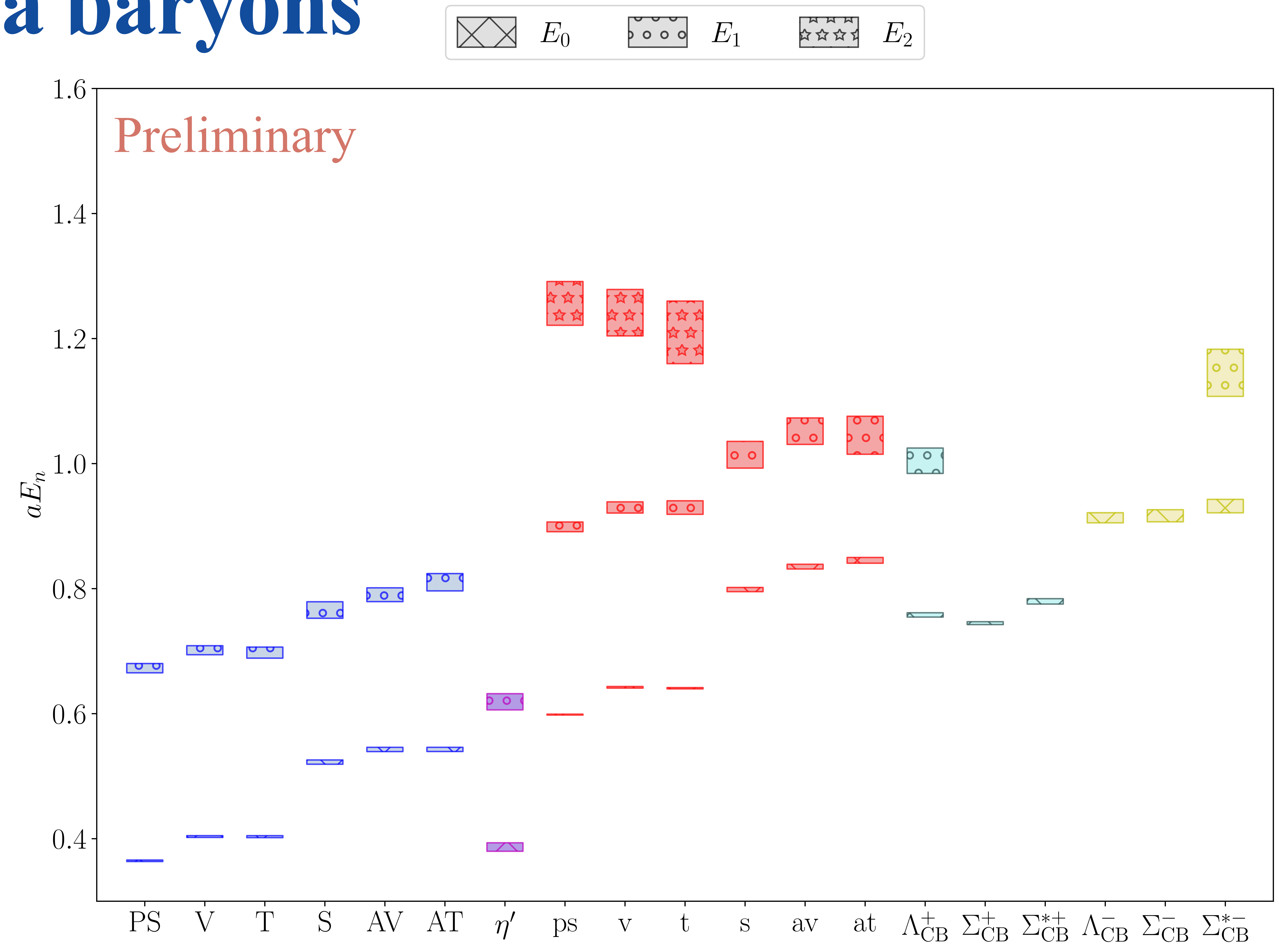

Results: chimera baryons

Dynamical simulations

Figure: spectrum of ensemble M5.

$(am_0^{(f)}, am_0^{(as)}) = (-0.72, -1.01)$

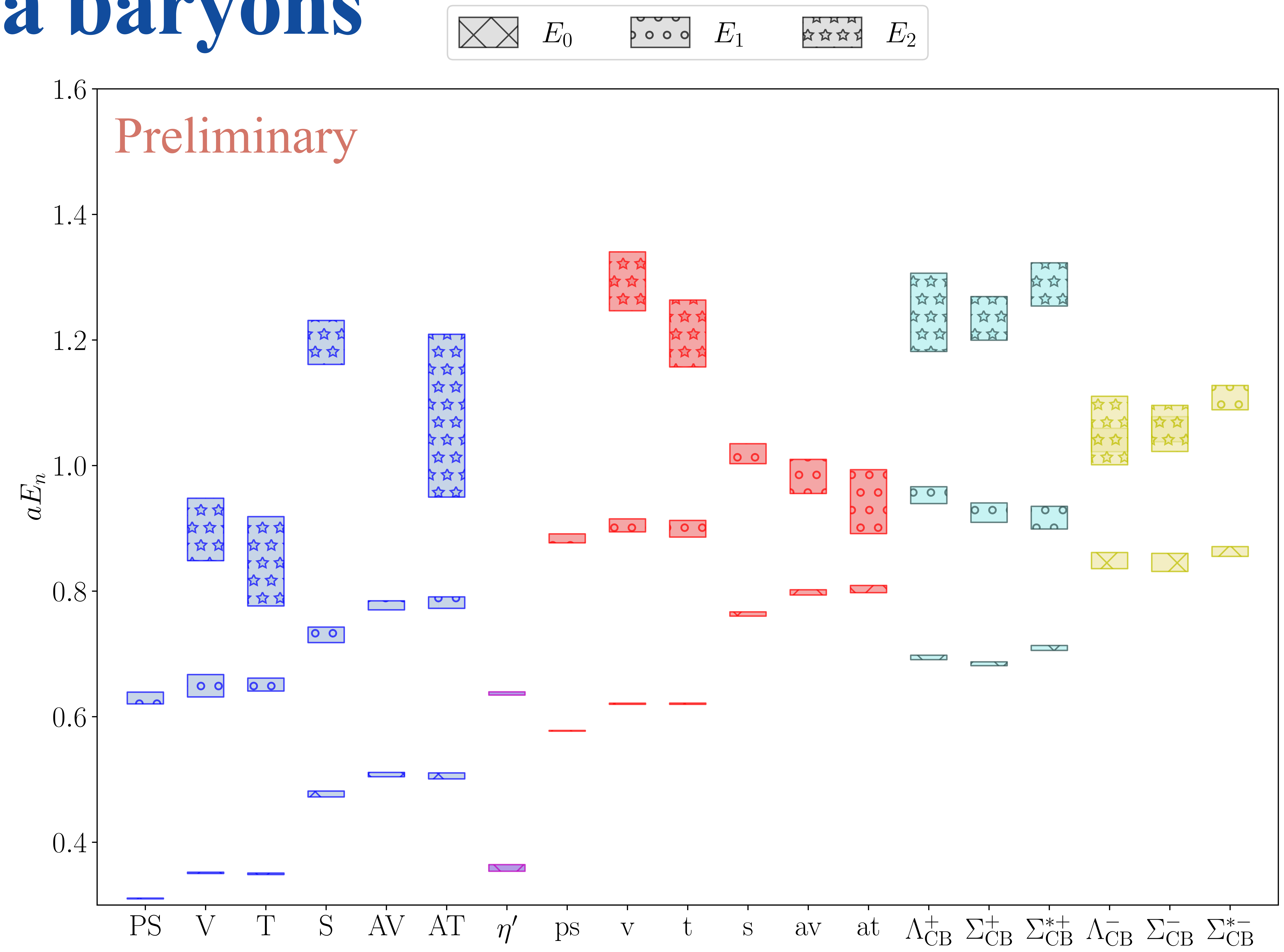

Summary and Outlook

- ☑ Composite Higgs model
- ☑ Mesonic spectra: quenched, F dynamical, AS dynamical (soon…)
- ☑ Chimera baryons
  - Λ and Σ: Top partner candidates in our model
  - Σ^* with spin-3/2
- ☐ Fully Dynamical studies

Outlook

Technical

- Changing the fermion action: clover fermion, DW fermion, …

Obserable

- Matrix elements of chimera baryons
- Four-hyperquark matrix elements

Theoretical

- Beta function: conformality
- Anomalous dimension of the top-partner interaction

END

Thank you

Backup slides

Results: Mesons

Smearing measurements

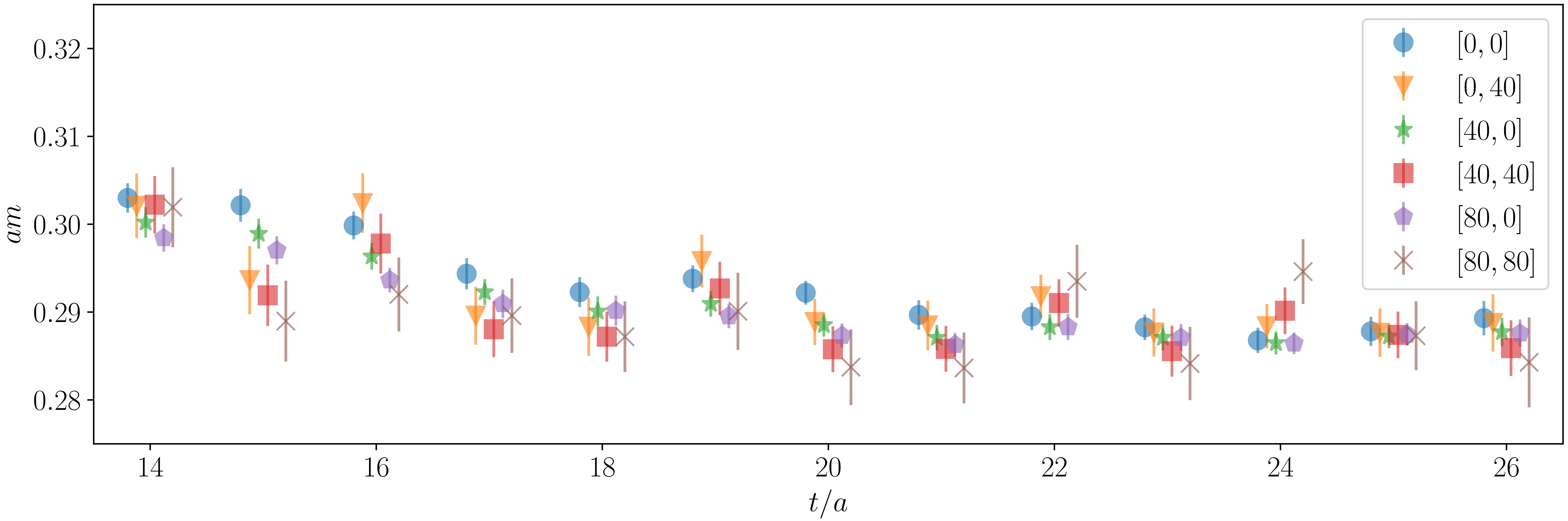

Figure: A demonstrative effective mass plot of the ps meson, measured on ensemble ASB4M5 with the lattice extents $N_t = 54$ and $N_s = 32$. Different colors (shapes) of dots represent various choices of Wuppertal smearing iteration numbers at the source and at the sink. The step size of Wuppertal smearing is fixed at 0.16 among all measurements. The APE smearing parameters are common in these measurements with $\alpha = 0.5$ and $N_{\text{APE}} = 50$.

Results: chimera baryons

Projection-CB two-point function

- Interpolating operator

$$\mathcal{O}^{\gamma}_{\mathrm{CB}}(x) \equiv \left(Q^{i\,a}{}_{\alpha}(x)\Gamma^{1\,\alpha\beta}Q^{j\,b}{}_{\beta}(x)\right)\Omega_{ad}\Omega_{bc}\Gamma^{2\,\delta\gamma}\Psi^{k\,cd}{}_{\gamma}(x)$$

- two-point function

$$\begin{aligned} C^{\gamma\gamma'}(t) &\equiv \sum_{\vec{x}}\langle\mathcal{O}^{\gamma}_{\mathrm{CB}}(x)\overline{\mathcal{O}^{\gamma'}_{\mathrm{CB}}}(0)\rangle \\ &= -\sum_{\vec{x}}\left(\Gamma^2 S_{\Psi}^{k\,cd}{}_{c'd'}(x,0)\overline{\Gamma^2}\right)_{\gamma\gamma'}\Omega_{cb}\Omega^{b'c'}\Omega_{ad}\Omega^{d'a'} \\ &\quad\times \mathrm{Tr}\left[\Gamma^1 S_Q^{b}{}_{b'}(x,0)\overline{\Gamma^1}S_Q^{a}{}_{a'}(x,0)\right] \end{aligned}$$

Results: chimera baryons

Projection-CB two-point function

- Interpolating operator

$$\mathcal{O}^{\gamma}_{\rm CB}(x) \equiv \left(Q^{i\,a}{}_{\alpha}(x)\Gamma^{1\,\alpha\beta}Q^{j\,b}{}_{\beta}(x)\right)\Omega_{ad}\Omega_{bc}\Gamma^{2\,\delta\gamma}\Psi^{k\,cd}{}_{\gamma}(x)$$

- two-point function

$$C^{\gamma\gamma'}(t) \equiv \sum_{\vec{x}}\langle\mathcal{O}^{\gamma}_{\rm CB}(x)\overline{\mathcal{O}^{\gamma'}_{\rm CB}}(0)\rangle$$
$$= -\sum_{\vec{x}}\left(\Gamma^2 S_{\Psi}^{k\,cd}{}_{c'd'}(x,0)\overline{\Gamma^2}\right)_{\gamma\gamma'}\Omega_{cb}\Omega^{b'c'}\Omega_{ad}\Omega^{d'a'}$$
$$\times\,\mathrm{Tr}\left[\Gamma^1 S_Q^b{}_{b'}(x,0)\overline{\Gamma^1}S_Q^a{}_{a'}(x,0)\right]$$

Parity projectors:

$$P_e \equiv \frac{1}{2}(1+\gamma^0)$$
$$P_o \equiv \frac{1}{2}(1-\gamma^0)$$

At large Euclidean time $\rightarrow P_e\left[c_e e^{-m_e t} + c_o e^{-m_o(T-t)}\right] - P_o\left[c_o e^{-m_o t} + c_e e^{-m_e(T-t)}\right]$

Results: chimera baryons

Spin projection

- Spin projector for Σ-type baryon:

$$\left(P^{3/2}\right)^{ij} = \delta^{ij} - \frac{1}{3}\gamma^i\gamma^j$$

$$\left(P^{1/2}\right)^{ij} = \frac{1}{3}\gamma^i\gamma^j$$

- Two-point function

$$C_{ij}(t) = \sum_{\vec{x}} \left\langle \mathcal{O}^i{}_{\mathrm{CB}}(x)\bar{\mathcal{O}}^j{}_{\mathrm{CB}}(0) \right\rangle \text{ with } \mathcal{O}^i_{CB} = \left(\bar{\psi}\gamma^i\psi\right)\chi$$

$$\rightarrow C^{1/2}_{\Sigma}(t) = \mathrm{Tr}\left[\left(P^{1/2}\right)^{ij} C_{jk}(t)\right]$$

Quenched ensembles

Ensemble	β	$N_t \times N_s^3$	$\langle P \rangle$	w_0/a
QB1	7.62	48×24^3	0.6018898(94)	1.448(3)
QB2	7.7	60×48^3	0.6088000(35)	1.6070(19)
QB3	7.85	60×48^3	0.6203809(28)	1.944(3)
QB4	8.0	60×48^3	0.6307425(27)	2.3149(12)
QB5	8.2	60×48^3	0.6432302(25)	2.8812(21)

Dynamical fundamental ensembles

Ensemble	β	am_0	$N_t \times N_s^3$	δ_{traj}	$\langle P \rangle$	w_0/a	am_{PS}
DB1M5	6.9	-0.91	32×16^3	20	0.55951(5)	0.9671(10)	0.4823(10)
DB1M6	6.9	-0.92	32×24^3	28	0.56204(3)	1.0375(16)	0.3868(12)
DB1M7	6.9	-0.924	32×24^3	12	0.56328(4)	1.07023(54)	0.34198(85)
DB2M1	7.05	-0.835	36×20^3	20	0.575267(29)	1.1881(18)	0.43797(99)
DB2M2	7.05	-0.85	36×24^3	24	0.577371(23)	1.2949(25)	0.32938(88)
DB2M3	7.05	-0.857	36×32^3	20	0.578324(13)	1.3580(14)	0.27256(69)
DB2M4	7.05	-0.863	36×36^3	16	0.579186(18)	1.4281(19)	0.2104(16)
DB3M3	7.2	-0.76	36×16^3	20	0.58767(4)	1.3898(26)	0.4698(11)
DB3M4	7.2	-0.77	36×24^3	20	0.588461(19)	1.4341(40)	0.42212(49)
DB3M5	7.2	-0.78	36×24^3	12	0.589257(20)	1.4980(11)	0.36992(64)
DB3M6	7.2	-0.79	36×24^3	20	0.590084(18)	1.5803(14)	0.31408(70)
DB3M7	7.2	-0.794	36×28^3	12	0.590429(9)	1.6154(11)	0.28585(49)
DB3M8	7.2	-0.799	40×32^3	12	0.590869(9)	1.6606(12)	0.2511(10)
DB3M9	7.2	-0.803	42×36^3	12	0.591226(6)	1.7156(15)	0.22063(52)
DB4M1	7.4	-0.72	48×32^3	12	0.604999(7)	1.9666(23)	0.32076(47)
DB4M2	7.4	-0.73	48×32^3	12	0.605519(7)	2.0519(30)	0.27119(44)
DB4M3	7.4	-0.74	48×36^3	12	0.606058(6)	2.1847(24)	0.21375(52)
DB5M1	7.5	-0.69	48×24^3	12	0.611900(13)	2.1484(72)	0.32600(73)

Dynamical antisymmetric ensembles

Ensemble	β	$am_0^{(\mathrm{as})}$	$N_t \times N_s^3$	δ_{traj}	$\langle P \rangle$	w_0/a	am_{ps}
ASB1M4	6.65	-1.07	48×24^3	16	0.587787(17)	2.5957(79)	0.41224(74)
ASB1M5	6.65	-1.075	48×28^3	12	0.589623(11)	3.057(10)	0.33700(80)
ASB1M6	6.65	-1.08	48×32^3	12	0.591451(10)	3.595(21)	0.25391(91)
ASB2M7	6.7	-1.055	48×24^3	12	0.590599(15)	2.6325(92)	0.42644(73)
ASB2M8	6.7	-1.06	48×24^3	12	0.592152(13)	2.908(11)	0.3627(11)
ASB2M9	6.7	-1.063	54×28^3	20	0.593154(13)	3.413(17)	0.3156(10)
ASB2M10	6.7	-1.065	54×32^3	12	0.593758(9)	3.607(12)	0.2862(10)
ASB2M11	6.7	-1.067	54×32^3	8	0.594443(7)	3.6981(84)	0.25826(66)
ASB2M12	6.7	-1.069	54×36^3	12	0.595063(7)	4.316(11)	0.22111(77)
ASB3M2	6.75	-1.041	54×24^3	20	0.593531(15)	2.6343(82)	0.43385(83)
ASB3M3	6.75	-1.046	54×24^3	12	0.595008(12)	3.079(13)	0.3697(10)
ASB3M4	6.75	-1.051	54×28^3	8	0.596339(10)	3.586(14)	0.30785(82)
ASB3M5	6.75	-1.055	54×32^3	8	0.597567(8)	4.056(12)	0.25347(44)
ASB4M3	6.8	-1.03	54×24^3	12	0.597270(13)	2.9382(84)	0.40463(85)
ASB4M4	6.8	-1.035	56×24^3	8	0.598552(10)	3.343(11)	0.34478(81)
ASB4M5	6.8	-1.04	54×32^3	8	0.599812(8)	3.705(14)	0.29058(92)
ASB4M7	6.8	-1.046	54×36^3	12	0.601392(7)	4.616(13)	0.21492(56)

Results: chimera baryons

Projection-Parity

$$C_{\mathrm{CB}}(t) \to P_e\left[c_e e^{-m_e t} + c_o e^{-m_o(T-t)}\right] - P_o\left[c_o e^{-m_o t} + c_e e^{-m_e(T-t)}\right]$$

- The log plot of the chimera baryon correlators (left) and their effective mass plot (right) with the parity projection.

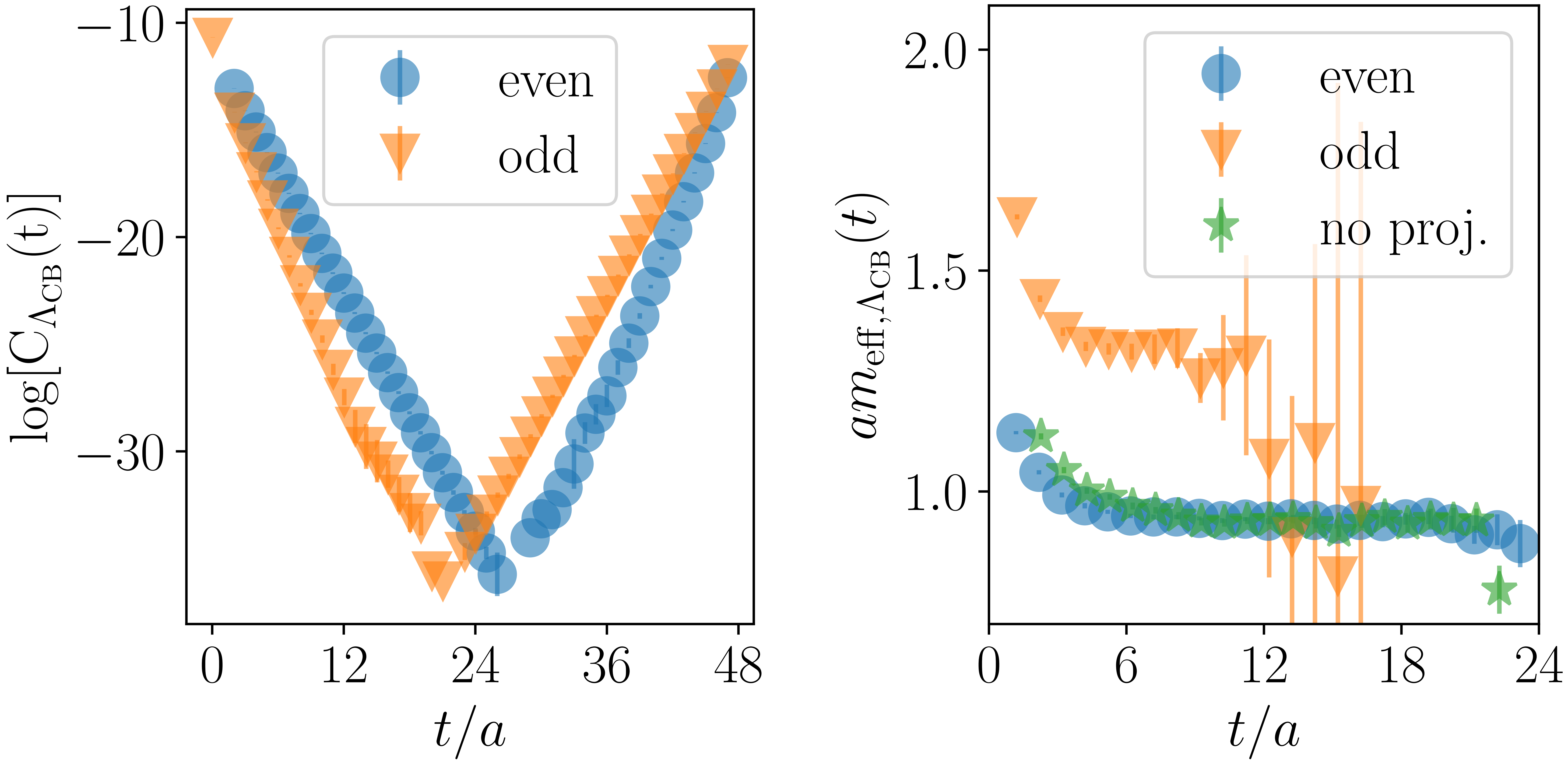

Results: chimera baryons

Massless-continuum limit

Figure: The mass of three chimera baryons, $\Lambda_{\rm CB}$, $\Sigma_{\rm CB}$, and $\Sigma^*_{\rm CB}$, as a function of $\hat{m}^2_{\rm PS}$ (left) and $\hat{m}^2_{\rm ps}$ (right), in the limit where the lattice spacing vanishes, while $\hat{m}^2_{\rm ps}=0$(left) and $\hat{m}^2_{\rm PS}=0$ (right).

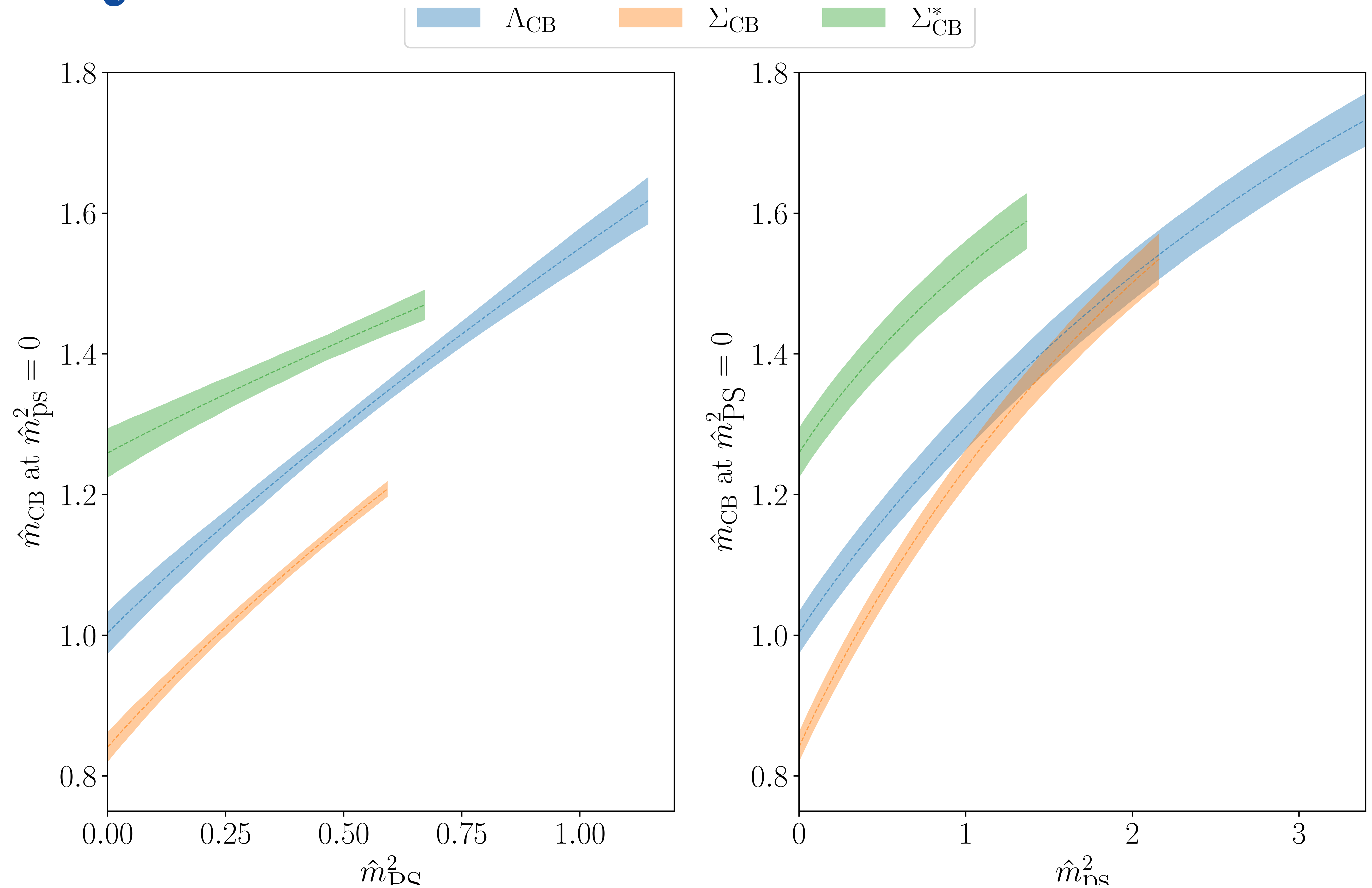

CB	Ansatz	$\hat{m}^\chi_{\rm CB}$	F_2	A_2	L_1	F_3	A_3	L_{2F}	L_{2A}	C_4
$\Lambda_{\rm CB}$	MC4	1.004(30)	0.692(67)	0.384(12)	-0.14(46)	-0.14(33)	-0.092(46)	0.091(76)	0.003(13)	-0.024(60)
$\Sigma_{\rm CB}$	MC4	0.842(21)	0.806(81)	0.558(13)	-0.14(33)	-0.24(68)	-0.162(77)	0.193(62)	-0.01(16)	-0.079(62)
$\Sigma^*_{\rm CB}$	M3	1.258(35)	0.36(10)	0.391(31)	-0.33(53)	-0.06(85)	-0.12(16)	0.335(86)	0.006(30)	-

Results: mesons

Dynamical simulations